2010

Emissions Characterization and Particle Size Distribution from a DPF-Equipped Diesel Truck Fueled with Biodiesel Blends

Idowu O. Olatunji
West Virginia University

Emissions Characterization and Particle Size Distribution from a DPF-Equipped Diesel Truck Fueled with Biodiesel Blends.

Idowu O. Olatunji

Thesis submitted to the
College of Engineering and Mineral Resources
at West Virginia University
in partial fulfillment of the requirements
for the degree of

Master of Science
in
Mechanical Engineering

Nigel N. Clark, Ph.D., Chair
Gregory Thompson, Ph.D.
John Nuszkowski, Ph.D.

Department of Mechanical and Aerospace Engineering

Morgantown, West Virginia
2010

Keywords: Biodiesel, Emissions, Exhaust Particles, Particle Size

Abstract

Emissions Characterization and Particle Size Distribution from a DPF-Equipped Diesel Truck Fueled with Biodiesel Blends.

Idowu O. Olatunji

Biodiesel may be derived from either plant or animal sources, and is usually employed as a compression ignition fuel in a blend with petroleum diesel (PD). Emissions differences between vehicles operated on biodiesel blends and PD have been published previously, but data do not cover the latest engine technologies. Prior studies have shown that biodiesel offers advantages in reducing particulate matter, with either no advantage or a slight disadvantage for oxides of nitrogen emissions. Literature also suggests that diesel engine exhaust particle number emissions are dominated by nucleation mode particles (NMPs) if present, while the mass emissions are dominated by accumulation mode particles (AMPs). This thesis describes a recent study on the emissions impact and exhaust particles size distribution and composition, under steady state condition, of a 2007 medium heavy duty diesel truck (MHDDT) fueled with two biodiesel blends, B20A and B20B, and PD. The truck was tested in a chassis dynamometer laboratory using three steady state driving cycles. The cycles include vehicle run at 20 mph for 30 minutes (MD1), 32 mph for 30 minutes (MD2) and 50 mph for 20 minutes (MD3). Emissions were measured using a full exhaust dilution tunnel equipped with a subsonic venturi and secondary dilution for PM sampling. A fast particle spectrometer (DMS 500) was used to measure the particle number concentration and size distribution from the vehicle exhaust.

The study showed that emissions were more speed dependent than fuel type. For any given cycle, the differences in CO_2 and NO_x tailpipe emissions produced by the PD, B20A and B20B were statistically insignificant with variations

of between 0.5-1.4%, and 0.5-3.4%, respectively at 95% confidence level. The results further showed that, for MD2, CO_2 emissions produced were lowest with corresponding highest fuel economy (miles per gallon (mpg) of fuel consumed). The NO_x emissions produced for B20A and B20B were slightly higher than those of PD, except for MD2. Generally, low particulate matter (PM) emissions were produced from the test results due to the truck diesel particulate filter (DPF). The carbon monoxide (CO) and hydrocarbon (HC) emissions were also low, with HC being difficult to quantify as a result of oxidation in the DPF.

Analysis of the exhaust particle data showed that, for all of the driving modes, the exhaust particles existed in two distinct modes with the particle number concentration dominated by the NMPs for all three test fuels. The particle mass concentration, dominated by the AMPs, substantially correlated with the pattern observed in the gravimetric PM mass emissions measurement. It was observed that factors such as DPF loading, dilution conditions (temperature, humidity) that are not fuel related strongly affected particle size formation especially in the NMP range. It was also observed that the total exhaust particle number concentration and the geometric mean diameter (GMD) increased with propulsion power. However, the GMD values were typically in the range of 25-40 nm for all driving modes and fuel type combinations. This is further confirmation that exhaust particles were dominated by nanoparticles that have been reported to cause respiratory diseases and other health effects in humans.

Acknowledgments

I am sincerely grateful to my advisor, Dr. Nigel Clark, for giving me the opportunity to realize my dream of pursuing a Master's Degree at WVU. Without your support, I am not sure if I would be able to get to this stage in life. Thank you for all the advice and motivation you have given to me. Thank you for trusting in me and also making me believe in myself. Dr. Gregory Thompson, you have made an enormous impact in my life. I thank you for all your advice and appreciate all what you have done for me. I am also thankful of the advice and support from Dr. John Nuszkowski for the time we have spent together.

I will also like to thank all of my colleagues and the staff of CAFEE for their support in completing this study. Special thanks go to Petr Sindler and Jason England for your help and expertise in collecting the data for this study.

To my parents and my siblings, I say thank you for believing in me, for all your prayers and for your words of encouragement. To my beloved wife, Oluwatosin, I thank you for all the love you have shown to me. Your support, understanding, endurance and motivation are most appreciated. I promise that I will always and forever love you.

Lastly, I give my utmost thanks to Almighty God, for His divine protection over my life up to this day and for making my dream come true.

Table of Contents

List of Figures

List of Tables

Nomenclature and Abbreviations

AMPs	Accumulation Mode Particles
ANR	Analyzer Rack
BER	Base Emissions Rate
BXX	Biodiesel Blend with XX% of Biodiesel
B20A	Biodiesel Blend with 20% of Animal Fat Biodiesel
B20B	Biodiesel Blend with 20% of Soybean Biodiesel
CAFEE	Center for Fuels, Engines and Emissions
CARB	California Air Resources Board
CLD	Chemiluminesecent Detection
CMPs	Coarse Mode Particles
CO	Carbon Monoxide
CO_2	Carbon Dioxide
COV	Coefficient of Variation
CVS	Constant Volume Sampler
DAQ	Data Acquisition
DMS 500	Fast Particle Spectrometer
DOC	Diesel Oxidation Catalyst
DOE	Department of Energy
DPF	Diesel Particulate Filter
EEPS	Engine Exhaust Particle Sizer
EGR	Exhaust Gas Recirculation
EMFAC	Emissions Factors
EPA	Environmental Protection Agency
FFA	Free Fatty Acid
ft-lbf	Foot – Pound Force
g/bhp-hr	Grams Per Brake Horsepower-Hour
g/mile	Grams Per Mile
g/sec	Grams Per Second

GMD	Geometric Mean Diameter
GREET	Greenhouse Gases, Regulated Emissions, and Energy Use in Transportation Model
HC	Hydrocarbon
HEPA	High Efficiency Particulate Air
HFID	Heated Flame Ionization
hp	Horsepower
IFC	Interface Unit
kW	Kilowatt
lb	Pounds
MCU	Main Control Unit
MD1	Drive Mode at 20 mph for 30 Minutes
MD2	Drive Mode at 35 mph for 30 Minutes
MD3	Drive Mode at 50 mph for 20 Minutes
MHDDT	Medium Heavy Duty Diesel Engine
mpg	Miles Per Gallon
mph	Miles Per Hour
NIDR	Non – Dispersive Infrared
nm	Nanometers
Nm	Newton – Meters
NMPs	Nucleation Mode Particles
NO_x	Oxides of Nitrogen
PD	Petroleum Diesel
PM	Particulate Matter
ppm	Parts Per Million
PSU	Power Supply Unit
SCR	Selective Catalytic Reduction
SHS	Sample Handling Unit
SI	Spark Ignition
SMPS	Scanning Mobility Particle Sizer

SO_2	Sulfur Dioxide
SO_3	Sulfur Trioxide
SOF	Soluble Organic Fraction
SSV	Subsonic Venturi
SVS	Solenoid Valve Unit
ULSD	Ultra Low Sulfur Diesel
VGT	Variable Geometry Turbocharger

1. Introduction

Reports of adverse health effects from the use of diesel engines [1 – 4] have generated concerns for regulators and decision makers around the world, despite the diesel engine's advantages of durability, better fuel consumption and efficiency than gasoline engines. In response, diesel engine emission regulations are becoming more stringent, particularly for particulate matter (PM) and oxides of nitrogen (NO_x) emissions. In the USA, the Environmental Protection Agency's (EPA) 2007 heavy-duty engine emissions standard represents an order of magnitude reduction in brake specific PM emissions from 0.1 g/bhp-hr to 0.01 g/bhp-hr (0.134 g/kW-hr to 0.0134 g/kW-hr) over the 2004 engine emissions standard. NO_x emissions were also reduced by 90% from 2 g/bhp-hr to 0.2 g/bhp-hr (2.68g/kW-hr to 0.268 g/kW-hr) in the 2007 EPA emissions standard over the 2004 emissions standard. The NOx emissions reductions were in phases over a period of 2007 to 2010. This required 50% of heavy-duty vehicles sold in the USA between 2007 and 2009 to meet the 0.2 g/bhp-hr while full compliance was enforced in 2010. Table 1 shows the EPA diesel engine emissions regulations for NOx and PM emissions since 1988 [5]. This could even become stricter in the near future. In addition to health issues, increased extraction and consumption of fossil fuels have caused declines in underground non-renewable petroleum-based resources [6]. This suggests that the world will be short of transportation fuel supply unless something is done to augment the ever-increasing world energy demand. Consequently, attention has focused on research in alternative fuel sources that can substitute for the depleting fossil fuel sources and that can possibly reduce the adverse health effects of diesel engine emissions.

Table 1: EPA diesel engine emissions regulations for NO_x and PM since 1988 [5].

Year	NO_x (g/bhp.hr)	PM (g/bhp.hr)
1988	10.7	0.60
1991	5.0	0.25
1998	4.0	0.10
2004	2.0	0.10
2007	0.2	0.01

Biodiesel, one of the viable alternative fuels, has the potential to displace 5% or more of PD market share in the next five or more years [7]. Biodiesel has the following benefits/properties which make it a good substitute for PD: it is renewable; it is non-toxic; it has excellent lubricity; it usually has higher cetane number than petroleum fuel; it produces lower CO_2, CO, HC and PM emissions compared to PD; It can be produced locally; and it can be used to power diesel engines without any need for engine modification.

Furthermore, a life-cycle assessment study done by Hong et al. [8] showed that biodiesel has less energy use and has lower emissions than PD. The study used the Greenhouse Gases, Regulated Emissions, and Energy Use in Transportation (GREET) model to assess the life-cycle impacts of biodiesel and PD. The GREET model revealed that, with biodiesel, it was possible to reduce fossil energy use and petroleum energy use by more than 52% and 88%, respectively, compared to PD. Biodiesel use could also reduce greenhouse gas emissions by more than 57% relative to PD. Biodiesel, chemically known as alkyl (methyl, ethyl or propyl) ester, is an oxygenated fuel produced from natural oils obtained from plant or animal source through a process called transesterification. Transesterification is a process by which plant oil or animal fat is chemically combined with excess alcohol in the presence of a basic or acidic catalyst to remove glycerin from the oil or fat molecular structure to make it suitable for use in a diesel engine [9]. Today, in the USA, biodiesel is being used to power diesel engines in blended form with PD. The biodiesel blends approved for use by USA diesel engine manufacturers are B5 and B6-20. B5's properties make it possible to

be used as a PD substitute without giving any performance-related problems [10]. B20 is the most commonly used biodiesel blend for two main reasons. First, it balances performance, emission levels, cost and availability. Second, B20 is the minimum blend level that qualifies as an alternative fuel in the USA, in line with the Energy Policy Act of 1992. Feedstocks for biodiesel production are obtained from edible and non-edible oil sources. Edible oils are obtained from species such as soybean, rapeseed, sunflower, and cotton, while non-edible oil sources include jatropha, honge, sea mango, and algae. However, more than 95% of biodiesel feedstocks come from edible oil sources because the properties of biodiesel produced from them are more suitable to be used as biodiesel [11]. Presently, biodiesel is mainly produced from soybean oil in the USA, canola or rapeseed and sunflower oils in Europe and palm and coconut oils in Asia [6]. This increases competition in the edible oil market and leads to high cost of edible oils and biodiesel [12]. As a result, researchers are focusing attention on biodiesel production from non-edible oils. A recent trend is biodiesel production from microalgae [13].

This thesis discusses a recent study on 2007 MHDDT using a chassis dynamometer testing laboratory. Tailpipe emissions, exhaust particle concentration and size distribution were characterized using two biodiesel blends, B20A and B20B, and PD. Comparisons were made among the three fuels to document, fuel or other effects on regulated and CO_2 emissions, exhaust particles size distribution and vehicle performance (in terms of fuel economy) of the MHDDT with an engine equipped with exhaust gas recirculation (EGR), diesel particulate filter (DPF) and variable geometry turbocharger (VGT).

2. Literature Review

In the USA and in Europe, diesel engine technology has evolved rapidly over the last two decades. In the early 90's, mechanically injected engines were replaced in the fleet with electronically managed engines. These engines had higher injection pressures, superior air management, and better in-cylinder charge motion than the previous models. However, these engines still relied largely on managing the start of injection for emissions control. Electronically managed waste gates for turbochargers were introduced, allowing for more control flexibility. To meet 2004 emissions standards, most manufacturers were obliged to employ EGR and advanced injection techniques for reduction of NO_x emissions. Engine management became substantially more complex as both EGR control and VGT control were needed. To meet 2007 PM emissions standards, engines were fitted with DPFs, and the regeneration of these units required further control sophistication. Also in 2007, the average NO_x emissions standard was further reduced [5], increasing the role of EGR in the combustion behavior. Little or no data exist for these late diesel engines in terms of performance and emissions using alternative fuel sources. Thus there is need for more testing to add to the available emissions and performance data inventory from alternative fuel sources, such as biodiesel, to help facilitate policy decision making. This chapter reviews the processes involved in the production of biodiesel from feedstocks and biodiesel use effects on engine emissions and performance. The chapter also reviews biodiesel and biodiesel blends effects on particle size distribution.

2.1. Biodiesel Production

Direct use of raw plant oils or animal fats in diesel engines has been shown to cause poor combustion, carbon build-up, choking, oil contamination that may result in engine failure in the long-term [14]. Hence the raw oils or fats need to be refined or processed to ensure engine durability. There are four different methods that can be used to produce biodiesel. These primary methods include micro-

emulsions, direct use and blending, thermal cracking (pyrolysis) and transesterification [15]. The transesterification process is the most widely used method because of its benefits over the others. The main purpose of transesterification is to reduce the viscosity of the plant oils or animal fats to a level that is comparable to PD so that the combustion properties of the oils or fats can be improved. The process involves a reaction between plant oils or animal fats (esters of saturated and unsaturated monocarboxylic acids with the trihydric alcohol glyceride) and alcohol in the presence of a basic, acidic or enzymic catalyst to improve the reaction rate [14,15]. The basic chemical reaction equation is shown in equation 1 below [15]:

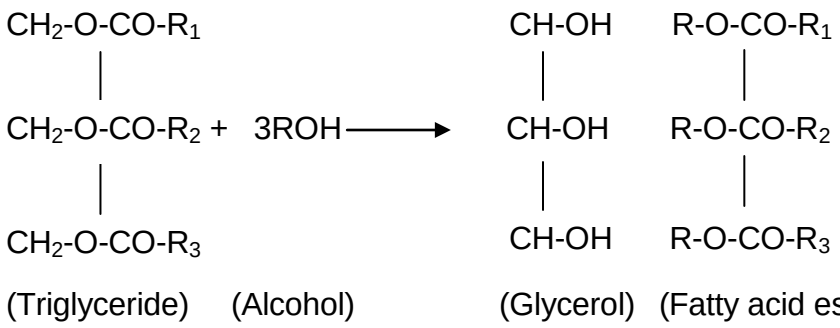

Equation 1

R1, R2 and R3 are long chain hydrocarbons called fatty acid chains. Methanol and ethanol are the most widely used alcohol for the transesterification reaction. However, methanol is preferred to ethanol because of its lower cost and its physical and chemical advantages. Sodium hydroxide and potassium hydroxide are the most commonly used catalysts in commercial transesterification process. The use of these basic catalysts is preferred because of their low cost and higher reaction rates compared to acidic and enzymic catalysts. The composition of the feedstock to be used for biodiesel production plays a role in the quality and yield of the biodiesel. Most biodiesel raw materials (feedstocks) usually contain triglycerides (esters), free fatty acids (FFA), water and other contaminants in various proportions [15]. A pretreatment is required for biodiesel feedstocks containing more than 2.5% of FFA by weight before transesterification process so that the biodiesel yield can be improved upon [16]. Methods of reducing or

removing FFA, water and other contaminants from biodiesel raw materials for high yield are detailed in reference [15]. It is also important to separate the fatty acid esters (biodiesel) from glycerol (by-product) after the transesterification reaction before purification and quality control processes. Refined glycerol may be used for manufacture of different industrial products such as medicines, soaps, moisturizers, cosmetics and other products [17-19]. Figure 1 below shows a process flow chart for biodiesel production using basic catalyst. Details of the various steps involved are well documented in reference [15].

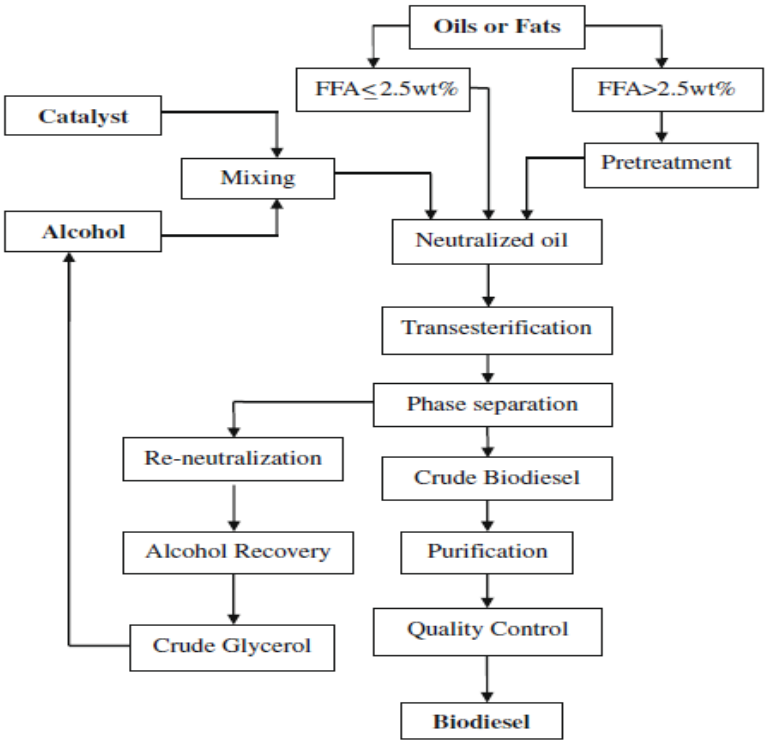

Figure 1: Chart showing the process involved in biodiesel production [15].

2.2. Biodiesel Emissions and Engine Performance Characteristics

It is generally agreed in the literature that the use of biodiesel and biodiesel blends in internal combustion engines reduces levels of some regulated emissions. Specifically, biodiesel use has been shown to reduce CO and HC emissions and substantially reduce PM emissions. However, while some investigators reported NO_x emissions increase with biodiesel use, others reported

NO_x emissions reduction when compared to that of PD. Engine model year, brand and technology have a big influence on the variability of NO_x emissions reported in the literature. The impact of biodiesel use on performance in diesel engines (i.e. fuel consumption and combustion characteristics such as injection timing, ignition delay, ignition temperature and pressure, heat release and combustion efficiency) has also been documented in the literature. Biodiesel is an oxygenated fuel, typically containing between 11% – 12% of oxygen by weight [20]. This and other physical and chemical properties of biodiesel such as viscosity, compressibility, cetane number, degree of unsaturation, density, etc, have been attributed for the unique behavior of biodiesel fuel. Following is a brief review of biodiesel use impact on engine emissions and performance.

In 2002, EPA produced a technical report that reviewed and published available biodiesel emissions data for heavy-duty engines. The summary of the report for regulated emissions is shown in Figure 2 below [21]. The report indicated that B20 use led to a reduction in PM, CO and HC emissions compared to PD. The report further showed that higher levels of reduction were possible with higher biodiesel blend percentage in the fuel. However, an overall average of 2% increase in NO_x emissions, which varied with biodiesel blend proportion, was also reported.

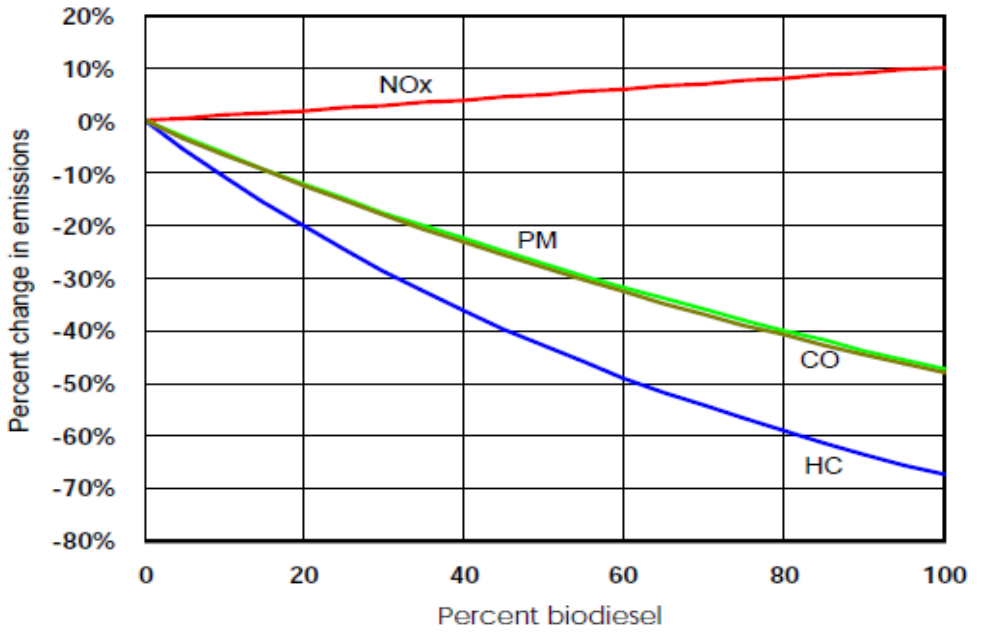

Figure 2: Biodiesel emissions impact for heavy-duty highway engines [21].

Wang et al. [22] investigated the effects of B35 (35% biodiesel and 65% PD) on emissions from two different heavy duty truck models tested in a chassis dynamometer testing laboratory using two driving cycles. The test results showed that B35 produced lower PM, CO and HC emissions than PD. NO_x emissions results were mixed: one truck with 1989 model engine (older) produced slightly higher NO_x emissions and the other with 1994 model engine (newer) produced slightly lower NO_x emissions, but the NO_x emissions changes were statistically insignificant compared to the PD. This suggests that the effects of engine design may have played a role in this. Lin et al. [23] compared the performance of biodiesel from eight different vegetable oil sources with PD in a single cylinder, DI diesel engine (YANMAR TF110-F). The results showed that the use of the biodiesel fuels produced a reduction of 50% to 73%, 22.5% to 33% in smoke and HC emissions, respectively, compared to PD. However, slightly higher NO_x emissions and fuel consumption were noticed, to varying degrees than PD, regardless of the biodiesel source. The study also showed that the use of biodiesel led to improved ignition quality because of its higher cetane number, and higher

combustion efficiency fuel due to its oxygen content, higher bulk modulus and better fuel atomization. Nabi and co-workers [24] conducted performance evaluation tests on a single cylinder, DI diesel engine using cotton seed oil biodiesel blends (B10, B20 and B30) and PD. The results showed lower PM emissions (24% reduction) were produced with B10 and 24% reduction in CO emissions with B30 compared to PD. Higher NO_x emissions and slightly lower thermal efficiency were noticed, which varied with the biodiesel blend proportion. The results of engine emissions tests performed by Mazumdar et al. [25] using biodiesel blends from waste cooking oil in a IDI diesel engine and Raheman et al. [26] using biodiesel from karanja (Pongamia Pinnata) oil in a DI diesel engine were largely in agreement except for NO_x emissions. Mazumdar et al. and Raheman et al. agreed and reported that biodiesel produced lower smoke, CO and HC emissions than PD. However, Mazumdar et al. showed that used cooking oil biodiesel blends produced higher NO_x emissions, while Raheman et al. reported that NO_x emissions decreased with karanja oil biodiesel. McCormick et al. [27] conducted tests in an engine laboratory on two direct injection engines inter-cooled with cooled high-pressure EGR, a 2002 Cummins ISB and a 2003 DDC Series 60, using PD and B20 as fuels. The B20 was obtained from four different feedstocks namely soybean oil, canola oil, yellow grease and beef tallow. The test results showed that, compared to PD, NO_x emissions increased slightly (by 3%) from the two engines with biodiesel blends, while PM emissions were significantly reduced by about 25%. Nine et al. [28] also conducted engine dynamometer testing on diesel–fueled marine engine (1972 Westerbeke 40) using blends of soybean biodiesel and PD. The “dry” (without water contact in the exhaust stream) emissions results revealed that pure biodiesel was able to reduce PM and CO emissions by 45% compared to PD. B50 and B100 resulted in 7% and 17% increase in NO_x emissions, respectively, compared to PD. The results of investigation of biodiesel impact on engine emissions done by McCormick et al. [29] and Nuszkowski et al. [30] were all consistent with the conclusions of most investigators above. Their results showed 10% – 35% reduction in PM emissions,

14% – 18% decrease in CO and HC emissions and a 2% – 4.3% increase in NO_x emissions in biodiesel blend (B20) emissions, as compared to PD. The investigation done by Thompson et al. [31] on biodiesel blends (B10 and B20) and PD fuel showed that variation in NO_x emissions were partially due to PD fuel properties relative to the biodiesel fuels properties. The result showed that NO_x increased with the biodiesel blends when their cetane numbers were significantly higher than that of PD. NO_x emissions reduction was also noticed when the PD fuel cetane number was closely matched with the neat biodiesel's cetane number.

The studies cited above clearly show that investigators agreed that the use of biodiesel produced low HC, CO and PM emissions. Moreover, the renewable nature of biodiesel has the potential to reduce dependency on PD as transportation fuel by at least 5% by 2015 [7] and reduce life cycle CO_2 emissions [32]. These benefits make biodiesel a viable substitute for PD. However, it is noticed that majority of the above reviews suggest that biodiesel use also produces slightly higher NO_x emissions than PD. This could limit the market penetration of biodiesel especially in the non-attainment areas, such as California and Texas, where strict NO_x emissions regulations are in effect. In view of this, research is now being focused on mitigating the NO_x emissions increase which results from the use of biodiesel. It is known that high temperature and oxygen promote formation of NO_x (thermal NO_x) in the combustion chamber by “Zeldovich mechanism” [33]. The properties of biodiesel, contribute to high temperature and pressure combustion in the combustion chamber through advanced combustion which promote NO_x formation. It is believed that some other mechanisms/effects could also affect biodiesel NO_x emissions. For instance, some biodiesel NO_x emissions reducing strategies, such as fuel additive for cetane improvement and injection timing retard, have been investigated for 2004 and older trucks. These strategies may not be effective for 2007 and newer trucks, and more research needs to be done. These NO_x reduction mechanisms/effects have not been fully understood and they are still been investigated so that an effective mitigating

mechanism can be put forward. The works of Mueller et al. [34], Thompson et al. [31] and Lapuerta et al. [35] provide a valuable insight to this line of research.

Two of the methods used to control engine NO_x emissions are the use of EGR and selective catalytic reduction (SCR). EGR involves recycling a portion of the exhaust gases into the combustion chamber. The recycled gases reduce the amount of oxygen and also serve as heat absorbers in the combustion chamber. The overall effect is to reduce in-cylinder temperature, which leads to reduction in thermal NO_x emissions. SCR uses hydrolysis-reduction principle to reduce NO_x emissions using urea which is stored as a separate fluid on the vehicle. EGR is commonly used in United States as a NO_x emissions mitigant while SCR is more popular in Europe. The effects of these devices on engine emissions are well documented in literature. For instance, Miller et al. [36] showed that NO_x engine-out emissions were reduced by over 70%, HC emissions by 100% reduction, PM by over 20% reduction with the use of urea-SCR after-treatment system. However, there was slight increase in CO emissions with the use of the urea-SCR system.

Although numerous studies showed that while EGR is effective in substantially reducing NO_x emissions, it also leads to increase in PM, CO and HC and CO_2 (measure of fuel consumption) emissions. The results of investigation done by Tsolakis et al. [37] using canola oil biodiesel blends in naturally aspirated diesel engine equipped with EGR showed that NO_x emissions decreased with increasing EGR rates. However, other engine emissions such as CO, HC and smoke (usually used as a measure of PM emissions) increased with increasing EGR rates. The results also indicated that the use of EGR led to increase in fuel consumption. The performance evaluation test conducted by Rajan et al. [38] revealed that HC and CO emissions increased with the use of EGR but with corresponding decrease in NO_x emissions especially at high loads. Because of the trade-off between NO_x and PM emissions with EGR use, it is usually used together with a DPF so that the increase caused by the use of EGR on PM, CO and HC can be mitigated. The combined use of EGR and DPF as an after-treatment system in

diesel-powered vehicles has been shown to be very effective in reducing all regulated emissions from diesel engines to below or at United States 2007 and Euro IV emissions regulation limits. Verbeek et al. [39] conducted performance evaluation tests on a DAF Euro IV heavy duty diesel engine equipped with both EGR and DPF. The results showed that the after-treatment system was an effective way to meet the emissions regulation applicable to the engine model year. Hohl et al. [40] tested Euro III and older engines retrofitted with EGR and DPF. The results showed that it was possible to reduce NO_x emissions by 50% while the filtration efficiency of the DPF for PM emissions reduction was greater than 99%. Chatterjee et al. [41] retrofitted the EGR-DPF system on 2000 and 2001 diesel-powered vehicles, which were tested on a chassis dynamometer. The results revealed that the system was able to reduce NO_x emissions by 50% - 60% and greater than 90% reduction in PM, CO and HC emissions. With 2007 NO_x emissions regulation fully enforced in 2010 in the United States, many engine manufacturers were obliged to improve their after-treatment solutions starting from their 2010 model engines to achieve the NO_x emissions target. One possible option is the use of an advanced EGR solution (EGR + DPF) system which is being used by Navistar International [42]. Other manufacturers are considering the use of urea + SCR with the existing system. Although the use of DPF technology has the tendency to reduce PM emissions by over 90%, questions still remain about the constituents of the PM emitted. The constituents are reported to be predominantly made up of particles of less than 50 nm in diameter that could pass through the filters of the DPF as a result of the DPF surface affinity.

2.3. Particulate Emissions from Diesel and Biodiesel Fuels

2.3.1. Particulates

In their report, Khair et al. [43] defines particulates, also known as PM, as particles present in combustion engine exhaust of an internal combustion engine that can be trapped on a sampling filter medium at 125^{o}F (25^{o}C) or less. While

particulates are emitted from both spark-ignition (SI) and diesel engines, a study by Johnson et al. [44] clearly showed that, on a one to one basis, particle mass and number engine-out emissions from diesel engines contribute significantly to atmospheric aerosols compared to SI engines. Hence PM emissions regulations have mostly targeted particulate emissions from diesel-powered engines. However, particle engine-out emissions from SI engines may have equal or even more significant effects on atmospheric aerosol because of the large number of SI vehicles on the road. Diesel exhaust particles are mostly composed of highly agglomerated carbonaceous and adsorbed materials, ash volatile and semi-volatile organic and sulfur compounds [45]. Typically, during combustion, locally rich regions promote the formation of solid carbon, much of which is subsequently oxidized and the remainder is exhausted as agglomerates [45]. In addition, a small proportion of atomized and evaporated lubrication oil escape oxidation and form the volatile or semi volatile organic compounds generally called soluble organic fraction (SOF) in the exhaust. In fact, Andersson et al. [46] showed in their study that sulfur and phosphorous contents of lubrication oil that enter the chamber during combustion contribute to the engine exhaust particles formation.

The SOF, formed from the fuel or/and lubrication oil, primarily contains polycyclic aromatic compounds having oxygen, nitrogen and sulfur atoms or molecules [47]. The sulfur content of the fuel/lubricant present in the combustion chamber is usually oxidized to sulfur dioxide (SO_2) while a small fraction is oxidized to sulfur trioxide (SO_3) [45]. It is the SO_3 that leads to the sulfuric compounds in the exhaust particle. Also the metallic compounds in the fuel and the oil are oxidized to form small amounts of organic ash that are usually present in the exhaust particle [45]. Figure 3 shows a typical particulate composition for a heavy-duty diesel engine tested under transient condition [45].The amount of each component present in a typical diesel engine exhaust is strongly affected by many processes including dilution conditions, cooling, adsorption, coagulation, collision, agglomeration, etc [48-53]. These processes determine the mass, number and size distributions of exhaust particles. For example, Abdul-Khalek et al. [53]

studied the influence of dilution and other conditions on exhaust particle size distribution measurements. They found out that particle size distribution and number measurements were strongly dependent on a host of measuring conditions such as dilution temperature and ratio, residence time, relative humidity and fuel sulfur content. When normal dilution conditions usually observed in the laboratory were varied, the change in particle concentration of up to two orders of magnitude was observed [53]. This suggests that particle dynamics is highly non-linear for exhaust particle measurements but strongly depends on conditions mentioned above. Hence there should be universal testing and measuring procedures to allow for comparison among studies. Efforts are underway to ensure this is achieved in future regulations [54].

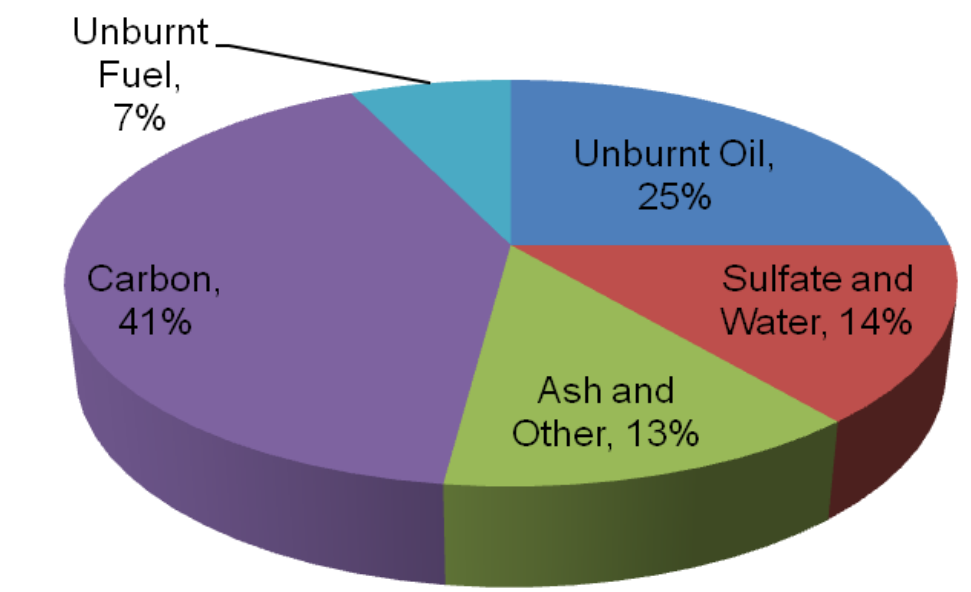

Figure 3: Constituents of a typical diesel engine exhaust particles [45].

2.3.2. Particle Size Distribution

Studies on particle size distribution of diesel particulates have received a great deal of attention from researchers and investigators in recent years. This is in anticipation that future emissions regulations are expected to cover restriction for particle size distribution and number concentration, most especially in Europe [54],

because current emissions regulations do not. The main reason for this is that various studies have shown that small exhaust particles cause adverse health effects and visibility problems [55]. It has also been shown that particle size distribution could not be inferred from mere measurement of particulate mass emissions [55]. It is generally agreed in literature that the current aftertreatment systems such as DOC-DPF and DPF only systems are very effective in reducing particulate mass emissions with filtration efficiency greater than 90%. More in-depth studies on aftertreatment systems revealed an increase in very small particle emissions from low-mass emission engines equipped the aftertreatment systems [56-60]. For instance, Kittelson and co-workers [56] performed on-road evaluation on two diesel exhaust aftertreatment (DPF). They found out that, although the DPFs were effective in reducing PM mass emissions, the DPF use led or could lead to production of large quantities of NMPs. The investigation conducted by Lee et al. [57] on a DPF equipped diesel engine revealed that most of the particles not trapped by the aftertreatment device were mainly ultrafine particles that are less than 100 nm in diameter. Abdul-Khalek et al. [58] showed that nearly all the number particle emissions produced downstream of a diesel engine equipped with ceramic filter are NMPs. The particle emissions were, however, strongly influenced by residence time. Meyer et al. [59] also studied the influence of different particulate traps on exhaust particle emissions. The result obtained was in agreement with [56] that large concentration of ultrafine particles were produced downstream of the particulate traps. However, a study by Baumgard et al. [61] showed that the increase in NMPs may not solely depend on aftertreatment systems' effect but also on the complexity of engine design. They tested a 1988 and a 1991 diesel engines using both ceramic particle trap and oxidation catalyst converter as aftertreatment system. The 1991 engine was designed for lower particulate mass emissions than the 1988 engine. The results obtained highlighted the differences between the 1988 and 1991 engines' exhaust particle size distributions. They concluded that the trap-equipped 1991 engine produced more NMPs and less AMPS than the trap-equipped 1988 engine when tested with the

same fuel. These very small diameter particles (nanoparticles) have been reported to have higher toxicity level because toxicity increases as particle size decreases [62]. In addition, nanoparticles have the higher tendency of inhalation and deposition in the respiratory system because of their very small size in the atmosphere. Hence, nanoparticles are likely to cause inflammation, respiratory disorder and other diseases [1-4, 62]. It is expected that better DPF technology will be developed in the near future that will be effective in reducing or suppressing PM mass emissions as well as particle number emissions.

Particle diameter is a commonly used metric to categorize size distributions of exhaust particles. Particle diameter can be expressed as Stokes diameter or aerodynamic diameter [63]. The diameter used would depend on the range of particle diameter of interest and the measuring instrument. Stokes diameter is usually used in size distributions based on light scattering and electrical mobility principles and it is independent of particle density. Hence it is appropriate for size distribution of small diameter particles in the range 1 nm to about 500 nm [63]. Aerodynamic diameter is density dependent and is mainly used to describe size distribution of particles with a diameter range greater than 500 nm. For example, aerodynamic diameter is used to describe size distributions resulting from the use of cascade impactors as the analyzer. In prior studies reviewed in the present study, majority of the size distributions were reported in Stokes diameter because of the particle diameter range involved with the exception of few that were reported in aerodynamic diameter.

Particle number emissions from diesel engine typically exist in tri-modal lognormal distribution form [45, 64-66]. These include the NMPs, AMPs and the coarse mode particles (CMPs) as shown in Figure 4. The NMPs (mostly described as nanoparticles) have diameter of less than 50 nm. The diameter of the AMPs typical ranges from 50 nm to 1000 nm and the CMPs have diameter greater that 1000 nm. The NMPs are primarily composed of semivolatile organic and sulfur compounds, elemental carbon, metallic compounds and other species. They could

make up to 20% of the total particle mass and more than 90% of the total particle number [64]. The AMPs, composed mainly of agglomerated carbon compounds and adsorbed materials, account for most of the particulate mass emissions. The CMPs are mainly re-entrained AMPs that were previously deposited on cylinder and exhaust system surfaces. CMPs typically make up 5-20% of the total particle mass [64]. Figure 4 shows a typical exhaust particle distribution in terms of number weighting, mass weighting and alveolar deposition fraction [64]. Note that in the figure, the concentration in any size range is proportional to the area under corresponding curve in that range. It is clear from Figure 4 that the NMPs dominate the particle number while AMPs dominate the particle mass. The alveolar deposition fraction relates to the deposition tendency of the particles and the pattern corroborated the fact that smallest particles are mostly inhaled and deposited in the respiratory tract.

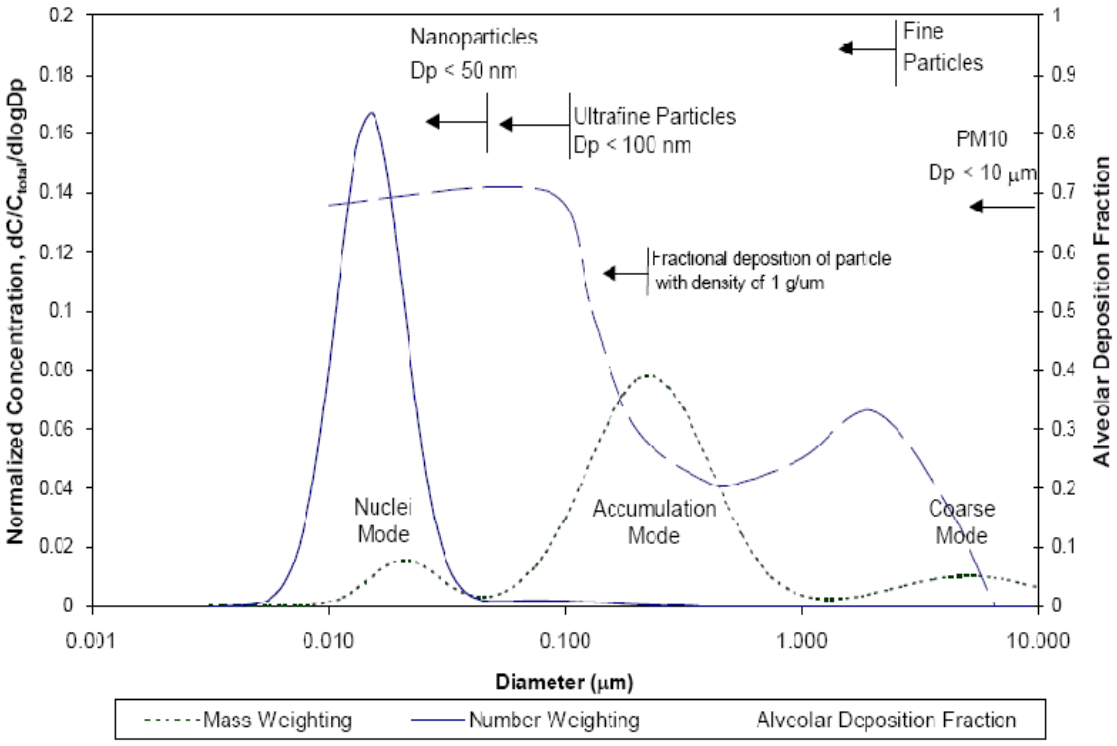

Figure 4:"Typical engine exhaust mass and number weighted size distributions shown with alveolar disposition fraction" [64].

2.3.3. Biodiesel Particle Emissions versus PD Particle Emissions

From the review of literature, it may be difficult to compare and conclude on which of the two fuel types (diesel and biodiesel or biodiesel blends) would produce less or more exhaust particles in one mode or the other when used in a diesel engine. This is because, as noted above, particle number and size distribution measurements are strongly dependent on the dilution and other conditions during measurement. This alone may introduce discrepancies and bias when comparing reports of different investigators and researchers. Various physical and chemical properties of biodiesel have been used by researchers to explain or justify both increases and decreases in the number of small exhaust particles emitted over that of PD. For instance, on one hand, the very low or no sulfur content of biodiesel may contribute to reduce the smallest particles since it is known that fuel sulfur content is associated and promotes the formation of the NMPs. On the other hand, higher viscosity and higher compressibility of biodiesel may lead to higher injection pressure, advanced injection process, reduce injection timing and advance combustion process all of which have been associated to an increase in the number of small particles in literature.

Nevertheless, the majority of researchers and investigators have reported increases in the number of small exhaust particles with biodiesel when compared to PD. Krahl and co-workers [67] conducted emissions comparison test on a DaimlerChrysler turbocharged diesel engine using pure canola oil biodiesel, PD and ultra low sulfur PD. The results obtained clearly showed an increased number of particles in the 10-40 nm diameter range, but a reduced number of particles above 40 nm range, when biodiesel was compared with PD. However, they also found a larger number of exhaust particles over the whole diameter range with ultra low PD when compared with biodiesel. Tan et al. [68] investigated exhaust particle emissions from turbocharged, Euro III diesel engine fuelled with PD and Jatropha biodiesel blends (B10, B20, B50 and B100). The exhaust particle number and size distribution were obtained using the Engine Exhaust Particle Sizer

(EEPS). The results revealed that the number of NMPs increases and the number of AMPs decreases with biodiesel when compared to the PD. The results further showed that the number of exhaust particles in each mode increases as the biodiesel blend ratio increases. Sinha et al. [69] conducted tests on a single cylinder, direct injection diesel engine equipped with EGR and fuelled with PD and biodiesel blends (B20, B40, B60, B100). The particle size distribution was measured by Scanning Mobility Particle Sizer (SMPS) at different injection pressures and a dilution ratio of 35:1. The results showed that all the biodiesel blends produced a higher number of NMPs and less AMPs when compared with PD at an injection pressure of 1200 bars. Jung et al. [70] examined particle emissions from a 1996 John Deere off-highway diesel engine using pure soy biodiesel and PD. They found that, with biodiesel, the particle number concentration of AMPs reduced by 38% resulting in a decrease in geometric number mean diameter in the same mode from 80 nm to 62 nm when compared to PD. Simultaneously, they found an increase in NMPs in terms of number concentration. The results of investigation conducted by Tsolakis [55] corroborated the conclusions of other investigators mentioned above. Tsolakis [55] found that, compared to PD, biodiesel produced lower particle mass emissions but higher number concentration of particles with low aerodynamic diameters when compared to the PD. Kim et al. [71] conducted emission performance evaluation of biodiesel using a common rail direct injection diesel engine equipped with aftertreatment device. The results showed that the particulate mass emissions were reduced with biodiesel blend compared to PD. However, the biodiesel blends produced higher particle number concentration for particles lower than 50 nm in diameter than the PD. Tinsdale et al. [72] carried out emissions tests on Euro IV diesel engine vehicle using biodiesel blends (B5, B10, B30) and PD over two drive cycle. The results obtained for engine exhaust particles indicated that biodiesel blends produced lower particulate mass emissions as a result of lower number of AMPs and higher number of NMPs produced compared to PD. The results further revealed that much more NMPs and much less AMPs were produced as biodiesel

blend proportion increased. Park et al. [73] analyzed exhaust emissions from a diesel engine fuelled with biodiesel blend (B20) and PD. They concluded that, compared to PD, the B20 produced a higher number of exhaust particles in the diameter range less than 50 nm (nanoparticles) and lower number of ultrafine and fine particles. Tan et al. [74] performed emissions tests on a direct injection, high pressure common rail diesel engine for passenger cars with jatropha biodiesel blends and PD. The analysis of the exhaust particle using Engine Exhaust Particle Sizer (EEPS) showed that the biodiesel blends produced higher number of NMPs but lower number of AMPs when compared with PD.

A number of investigators and authors agreed that biodiesel use produced less particulate mass but found no or insignificant increase in the number of small exhaust particles when compared to PD. For instance, Lapuerta et al. [75] measured particulate emissions from two different used cooking oil biodiesel fuels and PD. They obtained results that showed a decrease in the particle GMD with respect to that obtained from the PD. They contended that the decrease was due to a sharp reduction in the emission of AMPs rather than by an increase in the emissions of NMPs. The work of Bagley et al. [76] agreed with the conclusions of Lapuerta [75]. Bagley et al. [76] found a similar decrease in exhaust particle volume (mass) emissions with the use of soybean-oil biodiesel compared to PD. They concluded that particulate mass emissions were caused by up to 65% reduction of particles in the AMPs rather than by increase in the other particle modes. Some authors even found no significant effect of biodiesel use across the whole particle size diameter range although they agreed that biodiesel use produced less particulate mass compared to PD. Chen et al. [77] conducted tests on a single-cylinder engine under steady states conditions using soybean biodiesel and PD. They found that there was no significant difference in the GMD of the particle size distribution between biodiesel and PD fuels, although there were reductions both in mass and number of emitted particles with biodiesel use. Lapuerta et al. [78] examined particulate emissions from a diesel engine fuelled

with biofuels derived from vegetable oils and PD. They observed a sharp reduction in the number of particles emitted but not in their size distribution.

A few other reports suggested that biodiesel use actually produced a reduction in the number of smallest exhaust particles (NMPs). For instance, Aakko et al. [79] performed emissions evaluation on a bus diesel engine fuelled by canola oil biodiesel blends and PD. The results obtained showed that there was a decrease in the number of particles in the nucleation mode range with the biodiesel blends by using three different particle size distribution measuring instruments.

Finally, the review of literature showed that the use of biodiesel and its blends in compression ignition engines offer potential benefits over PD especially in terms of vehicle emissions (CO_2, CO, HC and PM), renewability and environmental impact. Particle number emissions advantage of biodiesel over PD is still unclear as this depends on many conditions, in addition to fuel effects, during measurement. Available literature data on biodiesel fuel performance mostly cover diesel engines and trucks of model year 2006 and earlier. Little or no biodiesel fuel use data exists for 2007 and later models of engines and trucks. The objective of this study is to add to the available data inventories on biodiesel use through the testing of a 2007 MHDDT in a chassis dynamometer laboratory. This could aid policy and decision makers to make informed decisions.

3. Experimental Set-Up and Procedures

The testing for the present study was conducted at one of the research laboratories of Center for Alternative Fuel Engines and Emissions (CAFEE) of West Virginia University located in Morgantown, WV. Specifically, chassis dynamometer testing for the MHDDT was done using the center's Heavy Duty Chassis Dynamometer Emissions Testing Laboratory located in the Industrial Park of Morgantown. This laboratory has fully transportable chassis dynamometers and a mobile container that were designed to meet EPA 2004 and 2007 and beyond emissions measurement specifications. The testing for the present study took place in November 2009. The procedure involved setting up a 2007 MHDDT, fuelled with biodiesel blends and PD, on a chassis dynamometer and measuring the regulated emissions (NO_x, CO and HC) and CO_2 emissions through the use of gaseous analyzers housed in the container. PM mass emissions were measured gravimetrically by collecting samples on filter that were later taken to an environmentally controlled mass measurement room. In addition to emissions characterization, exhaust particles were also measured in terms of number concentrations and size distribution in the range 5-1000 nm with the use of a Cambustion Fast Particulate Spectrometer (DMS 500).

3.1. Test Fuels

Three different fuels, namely PD, B20A, and B20B, were employed in this study. The PD was an ultra low sulfur diesel (ULSD) containing less than 15 ppm (parts per million) sulfur content. It was the recommended fuel for diesel engine use by EPA throughout the United States to help achieve the goal of meeting EPA 2007 PM emissions regulations. The PD used was obtained from part of the stock supplied by a local fuel delivery service (Guttman) to the laboratory at the time. Some of the physical and chemical properties of the PD are shown in Table 2 below. B20A was a biodiesel blend prepared by blending 20% by volume of biodiesel feedstock obtained from chicken fat with 80% (by volume) of the PD. The

biodiesel feedstock was 100% pure and was sold by Export Fuel Company (Export, Pennsylvania) and the certification sheet containing the property of the biodiesel provided by the seller. Similarly, B20B was prepared by blending 20% by volume of the biodiesel feedstock obtained from soybeans oil with 80% (by volume) of the same PD used in blending B20A. The soybeans feedstock was 99.9% pure with 0.1% PD. It was sold by Guttman Oil Company (Elkins, West Virginia) and the specification sheet provided by the company. The fuel blending was done gravimetrically at the CAFEE engine research laboratory. The process involved calculation of mass of each of the biodiesel feedstocks and the PD to make the required volumetric ratio using the specific gravities of the respective fuels and mixing them thoroughly. The specific gravity of each fuel was measured in the laboratory and was temperature corrected before being used in the blending calculation. The 0.1% PD in the soybeans feedstock was assumed to have the same properties as that of the PD used in blending. Samples of the biodiesel blends were sent for fuel properties analysis using ASTM D7467-09A test procedure. Some of the test analysis results are shown in Table 2. The complete fuel analysis report can be seen in the Appendix. It is noted that B20B does not meet the oxidation stability specification of 6 hours minimum. This, normally, should not affect the test results in any way as this specification only relates to storage capability for a certain period (6 months) before degradation sets in. The B20B was used a few days after being blended.

3.2. Test Vehicle

The test vehicle was a 2007 MHDDT manufactured by International Vehicle and Engine Corporation. The vehicle had a 2007 heavy duty diesel engine manufactured by the same manufacturer and meets EPA 2007 emissions regulation. The truck's engine was equipped with VGT and EGR. The engine was also equipped with DPF as an aftertreatment device. The test vehicle and engine details are shown in Table 3. Figure 5 also shows the MHDDT on the chassis dynamometer during testing.

Table 2: Selected properties of the fuels employed in this study.

Fuel Properties	B20A	B20B[1]	Petroleum Diesel
API Gravity (D 287)	37.1	37.8	39.1[2]
Cetane No. (D613)	51.8	59.4	52.5
Sulfur Content (D5453)	1.0 ppm	1.5 ppm	N/A
Flash Point P.M. (D93)	168^{o}F	170^{o}F	N/A
Cloud Point (D 2500)	12^{o}F	20^{o}F	N/A
Sulfated Ash (D874)	<0.001%	<0.001%	N/A
Viscosity (D445)	2.78 cST	2.24 cST	N/A
Oxidation Stability (EN 14112)	6.07 Hrs	3.18 Hrs	N/A

N/A – Not Available; B20A - Animal biodiesel blend; B20B - Soybean biodiesel blend; [1] biodiesel blend obtained from 99.9% soybean biodiesel feedstock; [2] based on measured specific gravity of 0.8293.

Table 3: Vehicle and engine details.

MY	2007
Manufacturer	International Truck and Engine
Model	Chassis
Odometer Reading (mile)	15053
Tire Size	245/75R22.5
Tire Diameter (inch)	38.2
Gross Vehicle Weight (lb)	25500
Curb Weight (lb)	10480 (without bed)
Engine Manufacturer	International Truck and Engine
Engine Model	GBT210
Engine Year	2007
Engine Peak Torque (ft-lb)	560 @ 1400 rpm
No. of Engine Cylinder	6
Transmission Type	Auto (Allison Transmission)
Transmission Speed	4

Figure 5: MHDDT used for this study.

3.3. Test Vehicle Parameters

Normally, before any vehicle testing is done on a chassis dynamometer, coast down procedures are usually performed with some known vehicle parameters. This is done to ensure that real life driving conditions are accurately simulated in the laboratory before the actual testing begins. In the coast down procedure, the actual road load of the vehicle is replicated on the dynamometer by using the pre-defined vehicle parameters. For the present study, the vehicle parameters used, which gave satisfactory results from the coast down procedure, are shown in Table 4. The vehicle speed was plotted against time for the actual coast down data. Figure 36 of the appendix shows some of the plotted data.

Table 4: Test vehicle parameters.

Test Vehicle Weight (lb)	23050
Drag Coefficient	0.665
Coefficient of Rolling Friction (μ)	0.00930
Frontal Area (sq. ft)	71

3.4. Drive Cycles

The vehicle was tested under steady state condition at the laboratory. Thus the vehicle was tested using three different steady speed schedules representing three different vehicle road loads. The steady speed drive cycles used were MD1, MD2 and MD3. The speed-time traces of the drive cycles are shown in Figure 6 below. It is important to say that each of the vehicle tests started after an initial warm up and after the desired vehicle speed was reached.

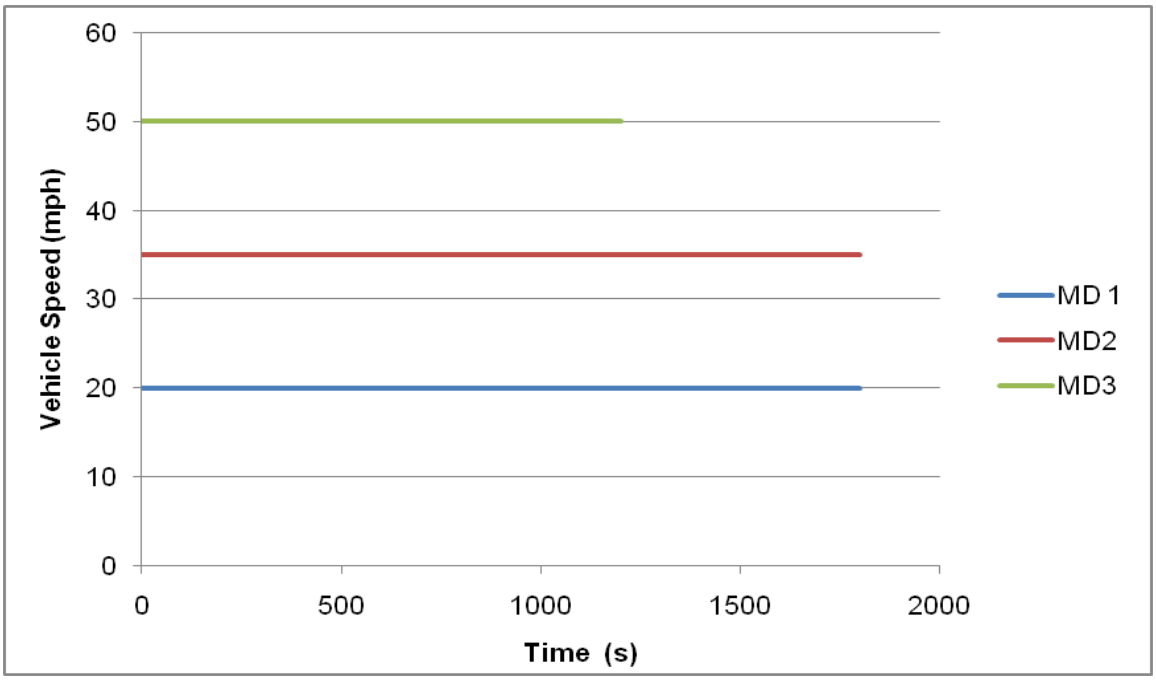

Figure 6: Time-speed traces for MD1, MD2 and MD3.

3.5. Chassis Dynamometer

Tailpipe vehicle emissions measurement requires the use of a chassis dynamometer alongside with other systems in order to quantify the emissions. Specifically, the test vehicle is usually set on a chassis dynamometer in order to obtain instantaneous mass emissions while the vehicle is being tested under realistic driving situations. Currently, CAFEE has dynamometers that are capable of simulating vehicle weight from 40,000lbs to 70,000lbs [80] and can be transported to clients' testing sites for use. One of these dynamometers was used

to test the 2007 MHDDT. The dynamometer bed consists of the ramp, two sets of rollers, joints, differentials, drive shafts, speed and torque measurement instruments (transducers), flywheel, motor and the power absorbers. The dynamometer was controlled by a Dyn-Loc IV digital dynamometer controller located at the data acquisition (DAQ) rack in the mobile container and integrated with test measurement system software. The test vehicle was rolled onto the test bed and hooked up to the dynamometer with the use of hub adapters by removing the outside rear tire on each side of the rear drive axle. The vehicle was held in place by the use of chains to help reduce vibration and tire slippage during testing. The other end of the hub adapters were attached directly to the dynamometer drive shafts to allow power to be drawn directly from the drive axle and to further reduce slippage. During testing, the vehicle drive axle's speed and torque were continuously measured and recorded to the DAQ. The flywheel was used to simulate the vehicle test weight. Figure 7 show the picture of the dynamometer used before the vehicle was loaded on it while Figure 8 shows the layout of the dynamometer.

Figure 7: Laboratory dynamometer bed.

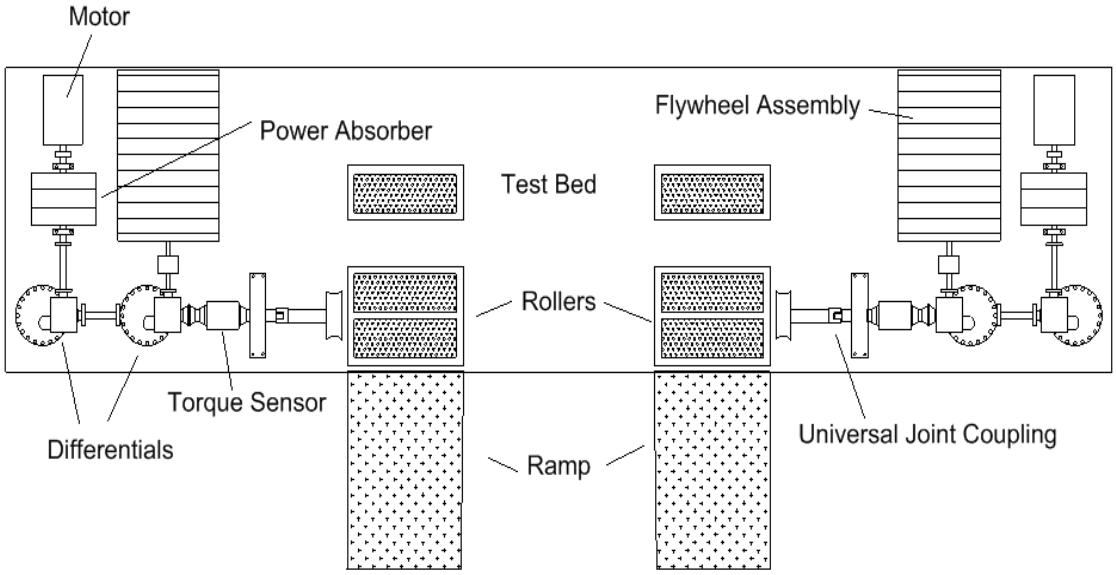

Figure 8: Layout of the chassis dynamometer [80].

3.6. CAFEE Mobile Laboratory

The newly constructed CFR 1065 compliant laboratory was used for the testing. The transportable laboratory is housed in a 30 foot long container. The mobile container houses the emissions sampling and measurement systems including two primary dilution tunnels, a subsonic venturi, a secondary tunnel for PM sampling and a gaseous emissions instrumentation system. The container also houses the HEPA primary dilution unit, an air-conditioning system, a chassis dynamometer control system, and a computer-based data acquisition and control system. Figure 9 shows an outside photographic view of the container. Figure 10 shows a 3-dimensional representation of the inside of the laboratory container [80].

Figure 9: Photographic view of the laboratory container.

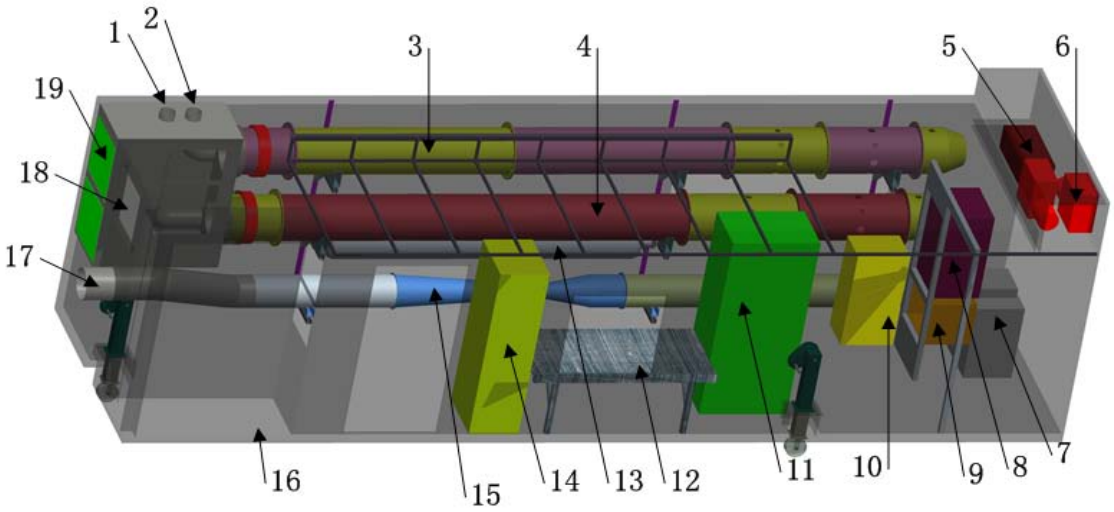

Figure 10: Three dimensional (3-D) representation of the laboratory container [80].

(1- Exhaust inlet of dirty tunnel; 2- Exhaust inlet of clean tunnel; 3- Clean tunnel; 4- Dirty tunnel; 5- Air compressor; 6- Vacuum pumps; 7- Oven; 8- PM sampling box; 9- Glove box; 10- Zero air generator; 11- MEXA-7200D motor exhaust gas analyzer; 12- Computer table; 13- Air tank; 14- DAQ rack; 15- Subsonic venturi; 16- Air conditioner deck; 17- Outlet to blower; 18- Ventilation fan; 19- HEPA filters)

As seen in Figure 10 above, the laboratory contains two primary dilution tunnels. Each dilution tunnel is of 18 inches ID and 20 feet long and was made of 316 stainless steel material. The primary dilution tunnels facilitate the measurement capability for both low emissions vehicles as well as traditional diesel-fueled vehicles. The upper tunnel referred to as the “clean tunnel” is used whenever low emissions vehicles are being tested. The “dirty tunnel” (lower tunnel) is usually used for the traditional diesel-fueled vehicles with high PM levels [80]. This arrangement helps to reduce tunnel history effects between test programs having different exhaust emission compositions. For the present study, the upper dilution tunnel was used since the vehicle was equipped with the DPF.

3.7. Vehicle Testing Sequence/Method

MD1, MD2 and MD3 were used as drive cycles for the vehicle testing using the three test fuels mentioned above. The test for MD2 using PD was repeated three times to demonstrate test repeatability and data capture consistency while all other tests were performed only once. The vehicle cruise control system was employed during testing to ensure steady speed operations except for the MD1 drive cycle. This was because the vehicle speed for MD1 was too low for the cruise control system operation. Hence the vehicle could not be held steady with the cruise control system at this speed.

3.8. Emissions Sampling System Method

The emissions sampling system principle of the laboratory is based on the subsonic venturi - constant volume sampler (SSV-CVS). The first step involved in emissions sampling was that raw exhaust from the vehicle was ducted towards the inlet of the primary tunnel through the use of transfer pipe. The raw exhaust was diluted with high efficiency particulate air (HEPA) filtered air just before the upstream of a mixing orifice with the mixture flow rate being controlled by the SSV – blower system situated at the end of the dilution tunnel. The streams were further mixed in the mixing region downstream of the 10-inch orifice plate [80]. The diluted

gaseous exhaust samples were collected by sample probes inserted at sampling plane located at approximately 10 times the tunnel diameter downstream of the mixing orifice, including samples for the PM analysis. The gaseous samples were then delivered to a Horiba MEXA 7200D motor exhaust gas analyzers and DMS 500 for quantification of the concentrations of CO_2, CO, HC and NO_x emissions and exhaust particles analysis, respectively. The PM sample was further drawn into the secondary tunnel, where it was diluted with more HEPA-filtered air, and passed through a cyclone separator. This was to separate particles that were greater than certain size in diameter (usually 10 µm). Figure 11 shows the schematic of the emissions sampling system [80].

3.9. Gaseous Emissions Measurement

As noted above, gaseous emissions samples were delivered to a Horiba MEXA 7200D motor exhaust gas analyzer system housed inside the laboratory container. The system is capable of measuring regulated emissions including NO_x, CO, THC and CO_2 emissions on a continuous basis. The MEXA system primarily consists of basic units namely the gas divider, the main control unit (MCU), the interface unit (IFC), the analyzer rack (ANR), the power supply unit (PSU), the solenoid valve unit (SVS), the sample handling unit (SHS) and the OVN-700 module [81]. The MCU is a computer system that houses the software that monitors and controls all other units of the system via the IFC which is the network/communication device. The ANR provides housing for the analyzer modules and can accommodate up to five analyzer modules. The SVS controls the flow of the operational and calibration gases to the analyzer modules while the SHS filters conditions and pumps the exhaust sample gas to the analyzer modules. Presently, three analyzers are fitted to the ANR. These include the AIA-721A CO analyzer, the AIA-722 CO/CO_2 analyzer and the CLA-720 “cold” NO_x analyzer. The OVN-700 module separately houses the FIA-725A THC and the CLA-720MA NO_x analyzers that need heated gaseous samples for proper operations. The AIA-721A CO and the AIA-722 CO/ CO_2 analyzers measure CO

and CO_2 emissions by using the non-dispersive infrared detection (NDIR) principle. The CO analyzer is capable of measuring between 50-5000 ppm range while the CO/CO_2 analyzer measures CO levels over 0.5-12 volume percent (vol%) and CO_2 levels over 3-20 vol%. The NO_x analyzer uses the principle of chemiluminesecent detection (CLD) to measure NO_x emissions. It is capable of measuring NO_x emissions over 10-10000 ppm range. The THC analyzer can measure emissions over 10-5000 ppm range and uses the heated flame ionization detection (HFID) principle. Figure 12 below shows the photo of the MEXA 7200D system

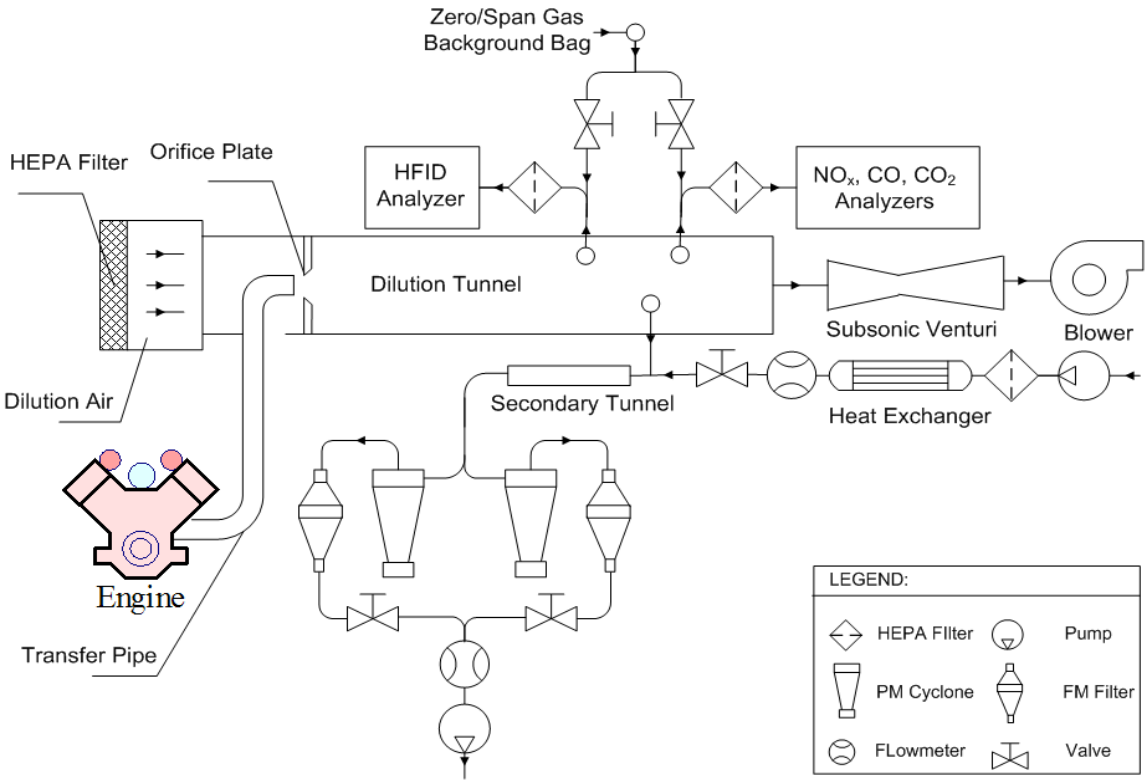

Figure 11: “Schematic of emissions sampling system” [80].

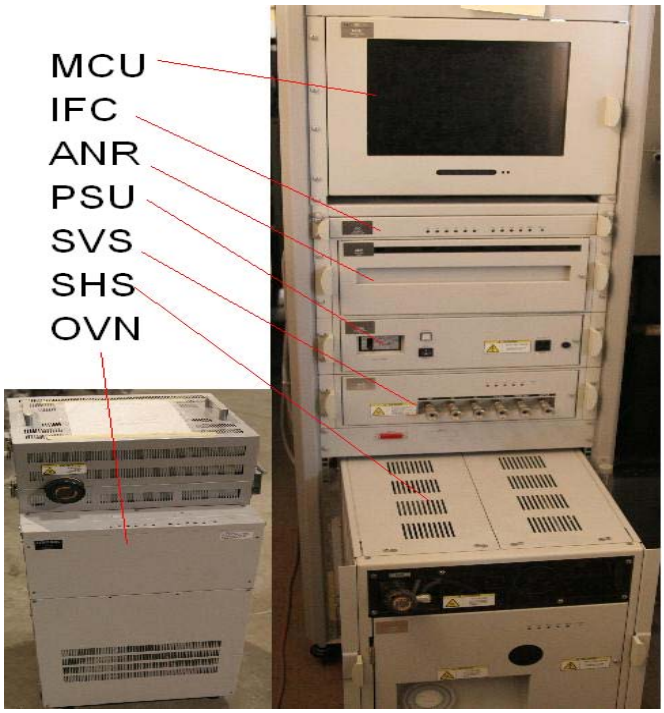

Figure 12: MEXA 7200D motor exhaust gas analyzer systems.

3.10. Secondary Dilution Tunnel and PM Sampling System

Gravimetric measurement of PM emissions is not completely determined in the laboratory but the sampling process is started during gaseous emissions sampling. The process is completed only after the masses of the PM filters are measured on a microbalance in an environmentally controlled room. For the present study, exhaust sample from the primary dilution tunnel was ducted to the secondary dilution tunnel maintained at 47°C where it was further diluted with treated air as required by the CFR 1065. At the end of the secondary dilution tunnel, the sample was drawn into a subsystem enclosure containing PM cyclone and PM filter holder where it passed through a pre-weighted TX-40 filter held in the filter holder. The enclosure temperature was maintained at 47°C so that the filter face temperature was within 47±5°C as stipulated in the CFR 1065. The filter was then carefully removed after testing and sent to class 1000 clean room for gravimetric analysis. Figure 13 below shows the diagram of the PM sampling subsystem showing the secondary dilution tunnel [80].

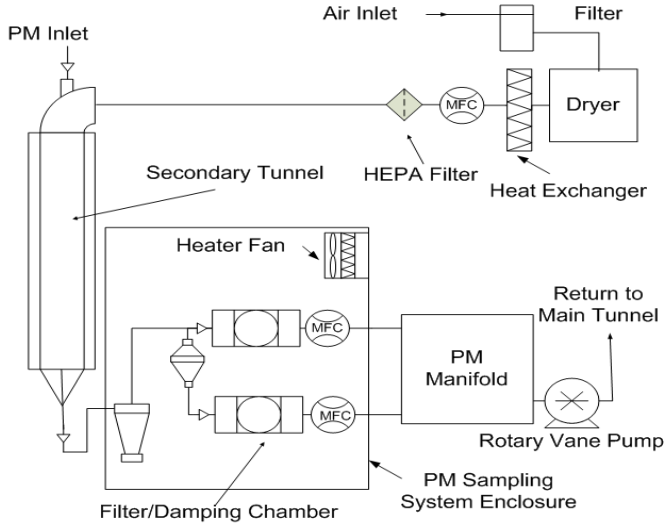

Figure 13: System for PM sampling [80].

3.11. Cambustion DMS 500 Fast Particle Spectrometer

DMS 500 was used to collect exhaust particles data during testing. This purpose was to quantify exhaust particle number concentration and size distribution so that comparisons could be made between PD and biodiesel blends' exhaust particles. In addition, the DMS 500 data analysis in terms of mass could also be used to validate the gravimetric PM emissions measurement. To achieve this, an assumption about the particle shape and density needs to be made. Some studies had assumed spherical particles with unit density for particle mass estimation [82]. Other studies developed empirical relationships to estimate mass of particles using the electrical mobility diameter of the particles [83]. In this report, the second approach was used for particle mass estimation. Electrical mobility property of particles is what is employed in the DMS 500 measuring principle. Electrical mobility is a measure of the ease of electric field deflection of charged particle and it is a function of charge on the particle as well as its aerodynamic drag. The DMS 500 instrument is capable of counting particles between 5 nm and 1000 nm electrical mobility diameter. The instrument operates by charging the particles that enter the instrument using a diffusion charging process. The charged particles then flow into a strong electric field contained in a classification column.

The electric field inside the column deflects the particles towards 22 electrometer detectors according to each particle's electrical mobility [84]. When the deflected particles impinge on the detectors, it results to changes in electrical current which can be measured and processed into spectral equivalent diameter and other desired particle data [84]. Figure 14 shows the picture of the DMS 500 with the data acquisition computer used to collect exhaust particle data during testing.

Figure 14: DMS 500 fast particle spectrometer.

3.12. Engine Control Unit (ECU) Data Collection

For each of the test runs, the vehicle engine performance data were collected. These include the ambient air temperature, current torque to maximum available torque, engine speed, coolant temperature and oil temperature. The performance data were collected via SAE 1587 communication protocol. SAE 1587 protocol is one of the heavy duty vehicle serial data communication standards that specify information sharing via datalink. Datalink is the process by which various subsystems of the vehicle communicate and share data among

themselves. The process involves conversion of information, in parallel form, from one subsystem to serial form for transport to other subsystems where the information is converted back to the parallel form [85].

Although engine performance data were collected, the actual engine torque and power demand could not be obtained from the data. The absolute torque data were not available because the lug curve required to do this could not be obtained from the engine manufacturer. However, the torque and power demand were estimated using the power available at the wheels to approximate the engine power with the assumption of 85% overall powertrain efficiency.

4. Results and Discussions

This chapter describes the emissions results and comparison among the three test fuels (PD, B20A, B20B) used for the present study. As noted in the previous chapter, tailpipe emissions from a 2007 MHDDT equipped with a 2007 turbocharged engine with EGR and DPF were compared for the three fuels. To arrive at these results and comparisons, three different steady state drive cycles (Figure 6) were used with a single test weight of 23050 lb. Regulated emissions including CO, NO_x, HC and PM together with CO_2 emissions and fuel consumption were reported and compared. All emissions were reported in the units of g/mile while fuel consumption data were reported in mpg.

In addition, exhaust particles' data obtained from the use of DMS 500 during testing were analyzed, reported and compared for the three fuels in terms of particle number concentration, particle GMD and particle mass concentration. Wherever applicable, particle mass concentration data were estimated by using the particle mass–diameter relationship previously developed and used by Symonds and co-workers [83]. The relationship is numerically defined as follows:

$$\text{Mass } (\mu g) = 1.54 \times 10^{-16} \times D^{3.19} \qquad \text{Equation 2}$$

D is the diameter of the particle in nanometers. Each of the particles' data was further analyzed to compare the number and mass proportions of NMPs, AMPs and CMPs. Finally, the gravimetric PM results and exhaust particles mass concentration results were compared with each other and the similarities and/or differences observed are discussed.

4.1. Statistical Analysis

The student t-test method was used to analyze differences in emissions results from the test data. All the statistical tests were done at 95% confidence level. To allow for the statistical computations, each of the single-run tests was divided into three time bins before being analyzed except for the test that had

repeat runs. It is noted that the t-test was performed on limited data using three data points and this may introduce some inaccuracies in the statistical results because of limited amount of data available for this study. For each of the exhaust particle data analyzed, GMD of the particles were obtained, reported and commented on in addition to particle number and mass concentration analysis.

4.2. Emissions Measurement Results

Before reporting the emissions results from the study, it is imperative to show or ascertain that the vehicle operation during testing was steady. To demonstrate this, continuous emissions measurement data (CO_2 and NO_x) from the three repeat runs using PD for MD2 were plotted against time. Figure 15 and Figure 16 show the variations in instantaneous CO_2 and NO_x emissions mass rate (g/sec) with time for the three repeat runs to show consistency of data collected at steady state conditions. These figures show that instantaneous emissions were fairly constant with time even though there was a high test-to-test variation (less than 11%) for NO_x emissions. Table 5 shows the integrated emissions data for the repeat runs with 1.2% and 10.8% variations in CO_2 and NO_x emissions measurement, respectively. The CO_2 data, with COV of 1.2% from run to run, imply that the engine fuel consumption and engine efficiency remained reproducible. However, NO_x emissions levels depend on many factors including in-cylinder EGR rates, the boost and back pressure, and the injection strategy among others. It is possible that changes in ambient conditions (Figure 17), or very small change in load, might result in different operating points for the EGR and for the turbocharger. Although variability in NO_x emissions would not be expected for legacy engines, the complexity of late model diesel engine controls can cause the type of variability seen in Figure 16.

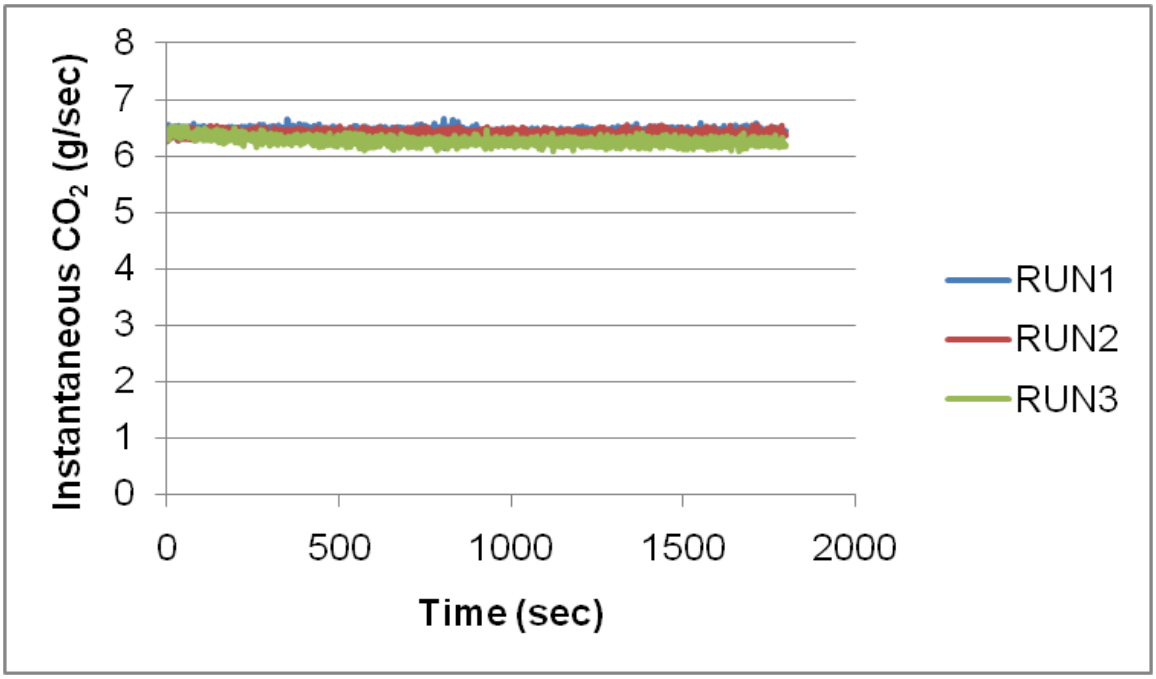

Figure 15: Instantaneous CO_2 emissions for three repeat runs.

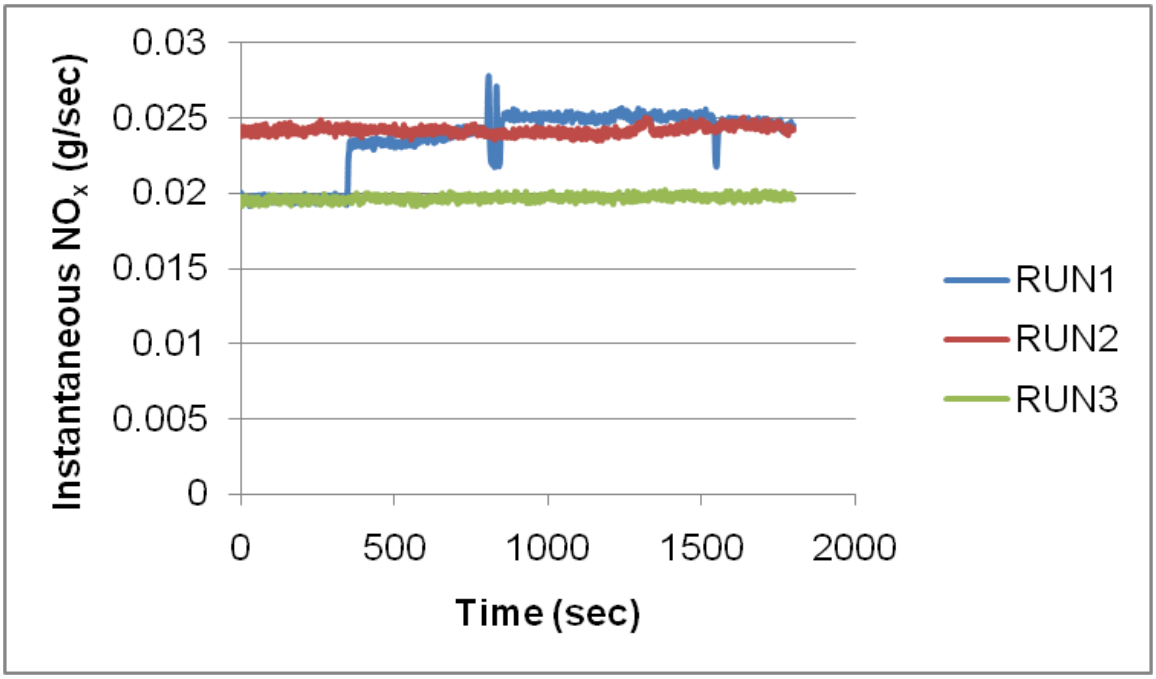

Figure 16: Instantaneous NO_x emissions for three repeat runs.

.

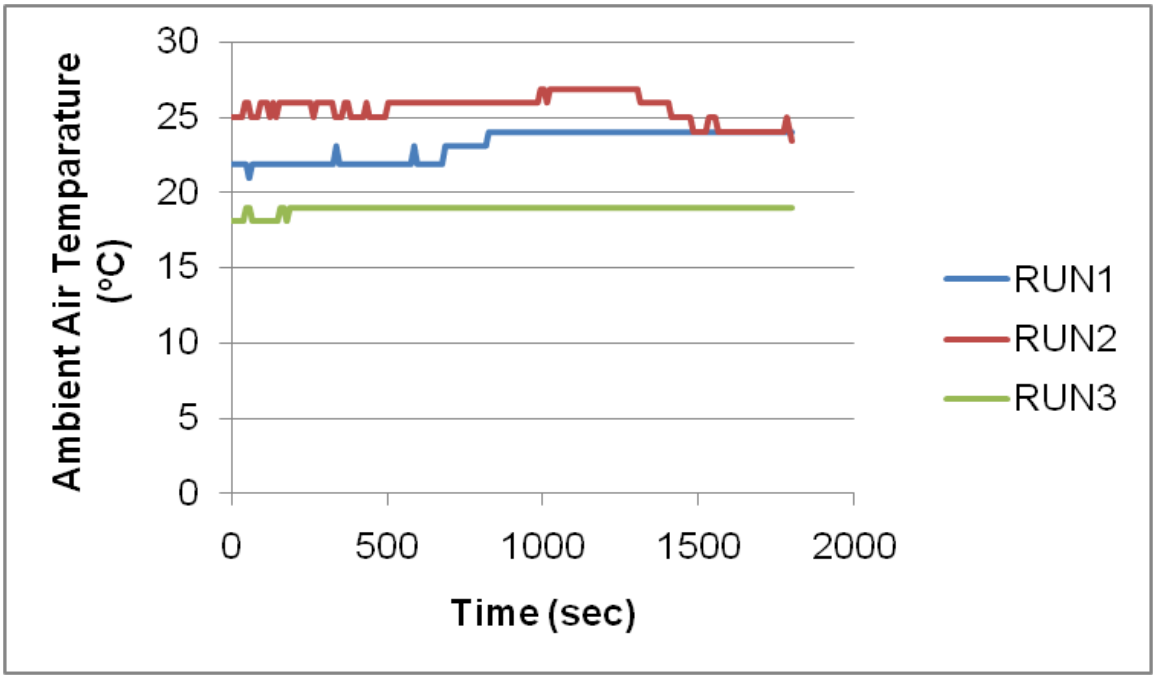

Figure 17: Variations in ambient air temperature during repeat runs.

Table 5: CO_2 and NO_x emissions data for repeat test runs

	CO_2 (g/mile)	NO_x (g/mile)
Run1	660.4	2.420
Run2	658.4	2.490
Run3	646.3	2.026
Mean	655.0	2.312
Std. dev	7.63	0.250
COV (%)	1.2	10.8

It is noted that the CO and HC emissions data were not analyzed for data consistency. This was because CO and HC emissions data showed a very high run to run variability because these emissions were of very low concentration for the trap equipped vehicle and consequently, very difficult to measure and quantify. The measurement accuracy for these emissions are further complicated by the combined effects of the vehicle EGR and DPF, fluctuations in engine load and measuring equipment resolution. It should also be noted that the effect of the engine fan operation may introduce some inaccuracies and uncertainty into the measurement of emissions.

For the single-run tests, each continuous data set was analyzed to ascertain any systemic change with time. Each of the data set was divided into three time bins and COV calculated for each bin. The purpose was to compare COV values of the three bins for a given data set with one another for each of the emissions species to determine the extent of data variation over time. Table 6 shows some data analysis for B20B representative of the extent of data variation in the other time bins for each of the emissions species based on the COV values. For instance, in the table, analysis from bin1 was shown for HC but represents the level of variation of HC emissions data in the other two time bins. Bin2 and bin3 data analysis were also shown for CO_2, NO_x and CO, which are also representative of data variation in the other two time bins for each of the emissions species. Similar data analysis trends (not shown) were observed for PD and B20A. Hence, it can be inferred that continuous data collected were steady with time basically for CO_2 and NO_x (with COV less than 10%) while the same could not be said of CO and HC. CO and HC continuous data showed very high variability with high COV as high as 206% and 620% respectively.

4.2.1. Vehicle Operating Parameters

The vehicle ECU data broadcast (engine speed), was used to infer the engine torque using the road load power requirement with 85% powertrain efficiency assumption. These estimations indicated that the vehicle operated at an

engine speed between 1370 rpm and 1500 rpm with an average engine torque of 60.9 ft-lbf for MD1. The high variability noticed in the engine speed was due to the fact that the cruise control system could not be used during testing. For the MD2, the engine operated at a speed between 1210 rpm and 1220 rpm with a corresponding average torque of 172 ft-lbf. Similarly, the vehicle operated at an engine speed between 1730 rpm and 1740 rpm with an average engine torque of 245 ft-lbf for MD3 (Table 7). As noted in the previous chapter, the vehicle cruise control system was used only during MD2 and MD3 testing. Figure 18 shows an instantaneous engine torque representative of vehicle operating condition for MD1, MD2 and MD3. Figure 18 showed that a lower variability in engine torque for MD2 and MD3 than MD1 during each testing. The average power requirements for MD1, MD2 and MD3 are 16.9 hp (12.6 kW), 39.8 hp (29.7 kW) and 80.8 hp (60.3 kW) respectively. Torque variations were more pronounced for MD1 because of the variability noticed in engine speed. This is attributable to the fact that the vehicle cruise control system could not be employed for MD1 testing.

Table 6: Variability of continuous emissions data for B20B.

	HC	CO_2	NOx	CO
MD1	Bin 1	Bin 2	Bin 3	Bin 3
Average (mg/sec)	0.0261	4643	13.0	0.0244
St. Dev. (mg/sec)	0.162	153	0.865	0.0501
COV (%)	620	3.3	6.7	206
MD2				
Average (mg/sec)	-0.105	6290	20.9	0.133
St. Dev. (mg/sec)	0.108	52.9	0.208	0.0636
COV (%)	-103	0.841	0.995	47.8
MD3				
Average (mg/sec)	-0.0367	13212	21.8	0.130
St. Dev. (mg/sec)	0.0716	98.9	0.576	0.0548
COV (%)	-195	0.749	2.64	42.1

Table 7: Average engine torque and power consumption for the drive cycles.

MD1		MD2		MD3	
Torque (Nm)	Power (kW)	Torque (Nm)	Power (kW)	Torque (Nm)	Power (kW)
86.2	12.6	233.2	29.7	332.2	60.3

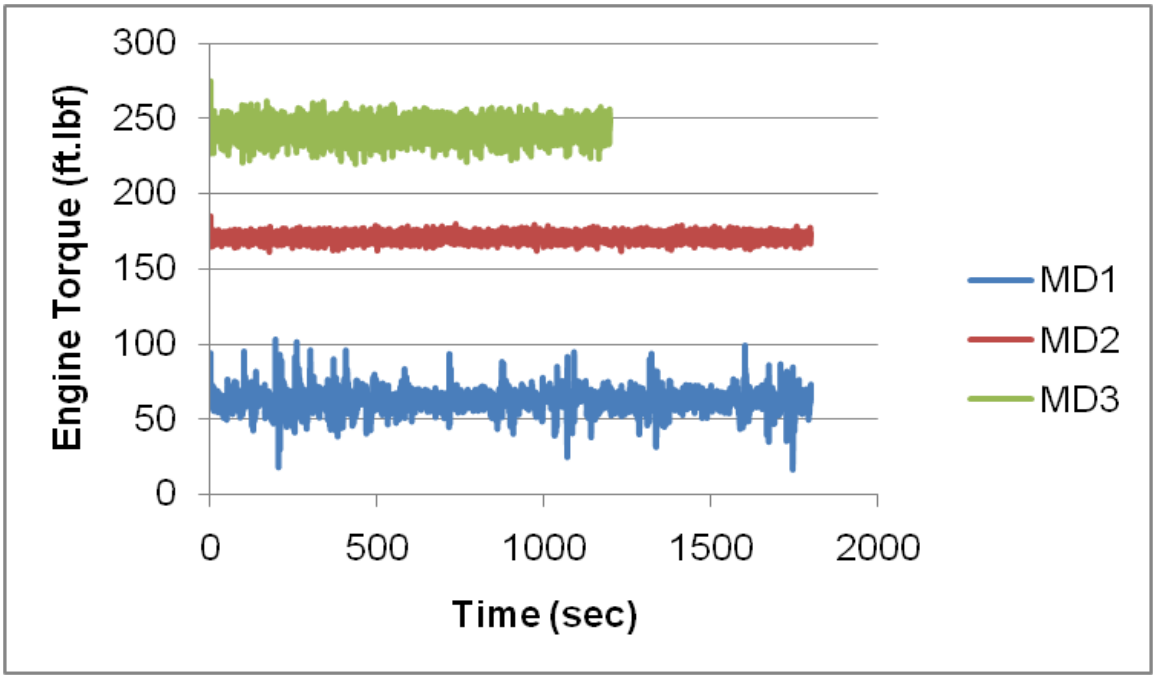

Figure 18: Plots of engine torque vs. time for the driving modes.

4.2.2. CO_2 Emissions and Fuel Economy

Figure 19 shows the variation of CO_2 emissions with the three test fuels for each of the drive cycle. The chart reveals that CO_2 emissions in the units of g/mile are vehicle speed dependent. The chart further reveals that, at any given speed, fuel type has little or no effect on CO_2 emissions as the same level of emissions were produced at a given vehicle speed which varied between 0.5% and 1.4%. Statistical analysis using a student t-test method at 95% confidence level showed

that the variations in emissions are insignificant, especially for MD1 and MD2. MD3 data analysis tended to show that statistically significant differences in emissions was evident among the three test fuels, but were still within the emissions variations mentioned above. This suggests that it could be possible to have marked differences in CO_2 emissions among the fuels at very high vehicle speed where more fuel is consumed. In general, all statistical analysis and error bars on the various charts were made possible by dividing the single-run continuous emissions data into 3 time bins. Fuel consumption, a metric for vehicle performance measurement, is related to the carbon content of the fuel. Therefore, it is noted in Figure 20 that at a given vehicle speed; the use of B20A and B20B produced lower fuel economy compared to PD. This is expected since PD typically contains high carbon content and no oxygen and thus higher heating value than biodiesel or biodiesel blends. This is consistent with the conclusions of many authors [23, 25] that less fuel is consumed with the use of PD compared to biodiesel blends because of the lower carbon content in biodiesel. Figure 20 represents fuel economy results from the test data. The fuel economy for PD was approximately 6% higher than the biodiesel blends for all the drive cycles. The carbon compositions of the fuels were estimated to be 87%, 84.7% and 84.8% by mass for PD, B20A and B20B respectively. The estimated carbon content of the biodiesel blends suggests that B20B may have the same or slightly higher fuel economy than B20A. This is evident in Figure 20 especially for MD2 and MD3. MD1 may not truly represent the differences in fuel economy among the fuel of the driver variability since cruise control was not employed for MD1 testing. It is also clear that the vehicle has better fuel economy at MD2 than at MD1 and MD3. This is expected because at light load (20 mph), engine is less efficient. In addition, any small changes in engine load with time detract from low vehicle speed efficiency. Inherent losses associated with low speed operations result in high fuel consumption. High fuel consumption also results at very high speeds (50 mph) when aerodynamic drag dominates the power requirement for propulsion. Thus, it can be concluded that the test truck would consume least amount of fuel at an

"intermediate" speed between a low speed and a high speed that balances the two factors mentioned above. In this case, the "intermediate" speed appeared to be around 35 mph. The above assertion is corroborated by the CARB (California Air Resources Board) report on the carbon dioxide emissions modeling and fuel economy estimation [86].

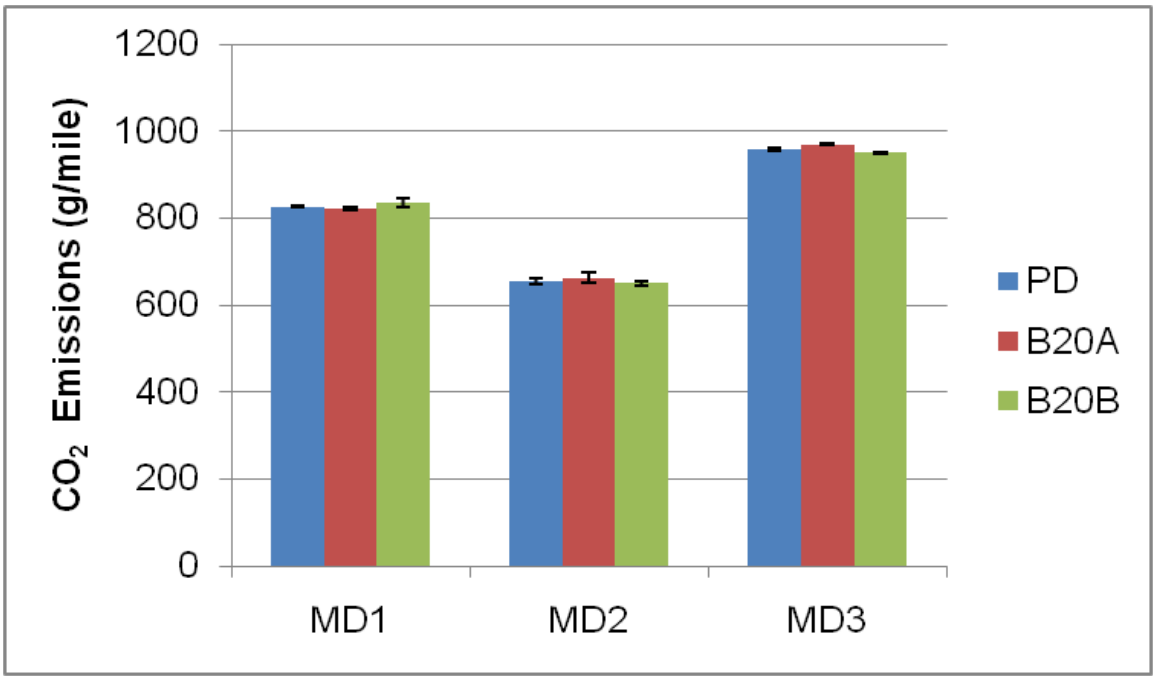

Figure 19: CO_2 emissions comparison for the test fuels.

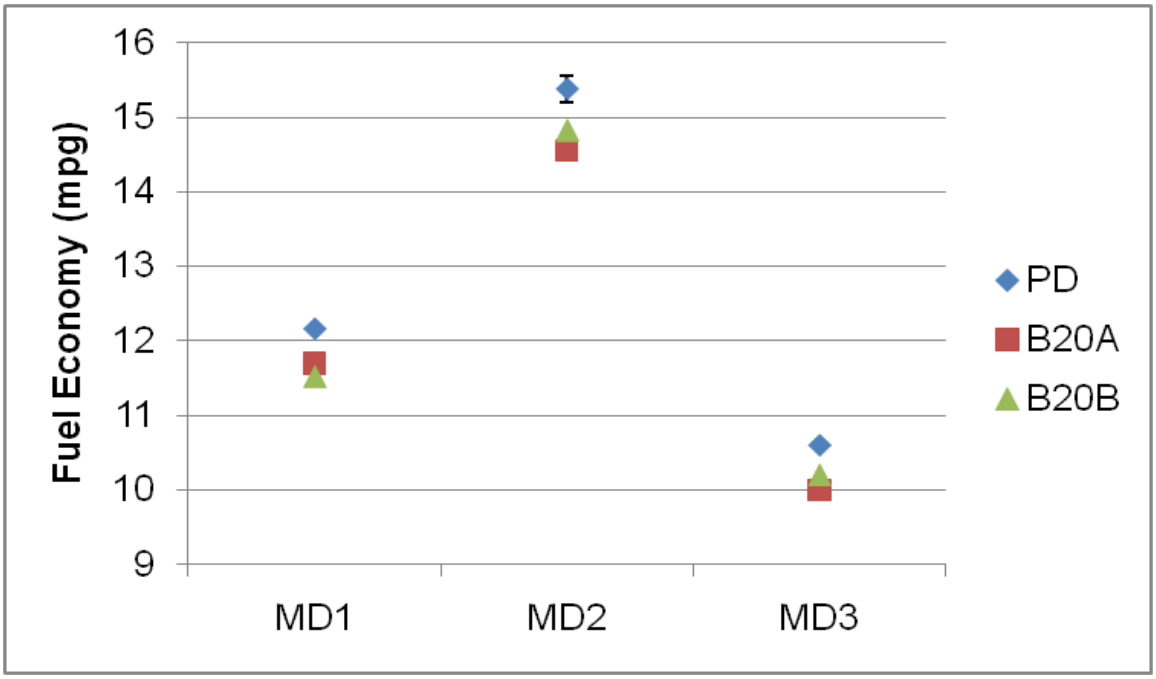

Figure 20: Fuel economy comparison for the test fuels.

4.2.3. CO Emissions.

The CO emissions obtained from the test data are displayed in Figure 21. It can be observed that PD produced lower CO emissions than the biodiesel blends, while B20A produced relatively higher CO emissions than B20B for all tests. It has to be noted that the level of CO emissions concentrations from the tests were approximately at the same level as the background CO concentration. The low CO emissions concentrations are attributable to the oxidation action of the DPF during testing. The low concentration, as a result of the DPF action, makes it difficult to accurately quantify the CO emissions and the measurement accuracy is further complicated by the slight fluctuations in engine load. A comparison can be made between the levels of CO emissions of this study with CO emissions from older trucks to see the effects of the DPF. Specifically, this can be compared with CO emissions from 2001 medium heavy duty diesel truck manufactured by Navistar International Truck Company. The 2001 truck emissions data were obtained from CRC Report No. E55/59 (page 304 of the Appendix to the report) by Clark et al. [87]. The report shows that the 2001 non-DPF truck emitted 0.97g/mile of CO

emissions, compared to between 0.015 g/mile to 0.02 g/mile for the 2007 truck equipped with both EGR and DPF. One reason for the reduction and the emissions pattern is the oxidation effect of the truck's DPF. The high variability in the instantaneous emissions pattern for CO suggests that factors other than the fuels may have contributed to the emissions pattern noticed in Figure 21. Although factors such as EGR action and multiple injections may marginally affect CO emissions, the effect of the DPF is far more dominant. The operation of the DPF is usually influenced by the exhaust temperature and DPF's loading. With the loading of the DPF changing with time, it would be difficult to maintain repeatability from run to run with DPF-equipped vehicles especially for emissions types such as CO and HC that are oxidized in the DPF. Another factor that could contribute to the high variability in CO emissions is ambient conditions. Consequently, the emissions pattern of Figure 21 was probably due to the DPF action and not the fuels.

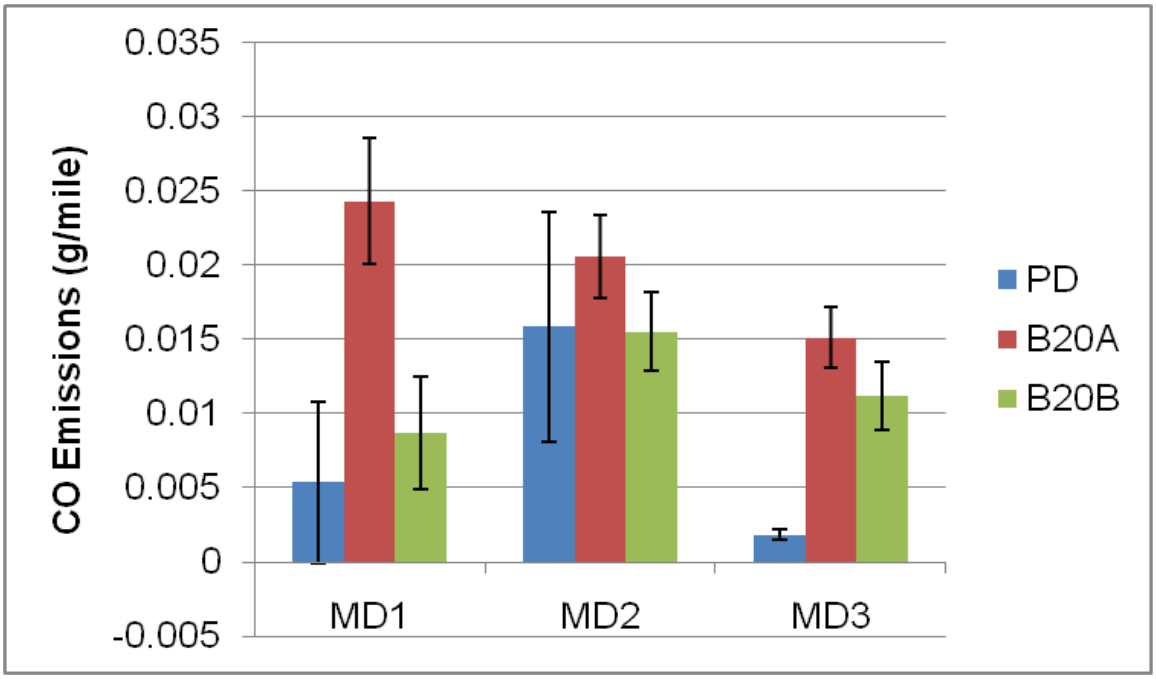

Figure 21: CO emissions using three driving cycles and test fuels.

4.2.4. HC Emissions

The HC emissions obtained from the test data are shown in Figure 22. As it can be seen in the figure, the tunnel HC emissions concentration levels were at or slightly higher than the background HC levels. In fact, some measured concentration levels were even below the background levels resulting in negative emissions shown in the figure. The low concentration levels, due mainly to the DPF oxidation effects, make it difficult for the HC emissions to be accurately quantified. In addition, the quantification process has been made complicated by fluctuations in engine load and equipment resolution resulting in no definite pattern in Figure 22. Consequently, fuel effects on HC emissions could not be easily ascertained just as in the case of CO emissions.

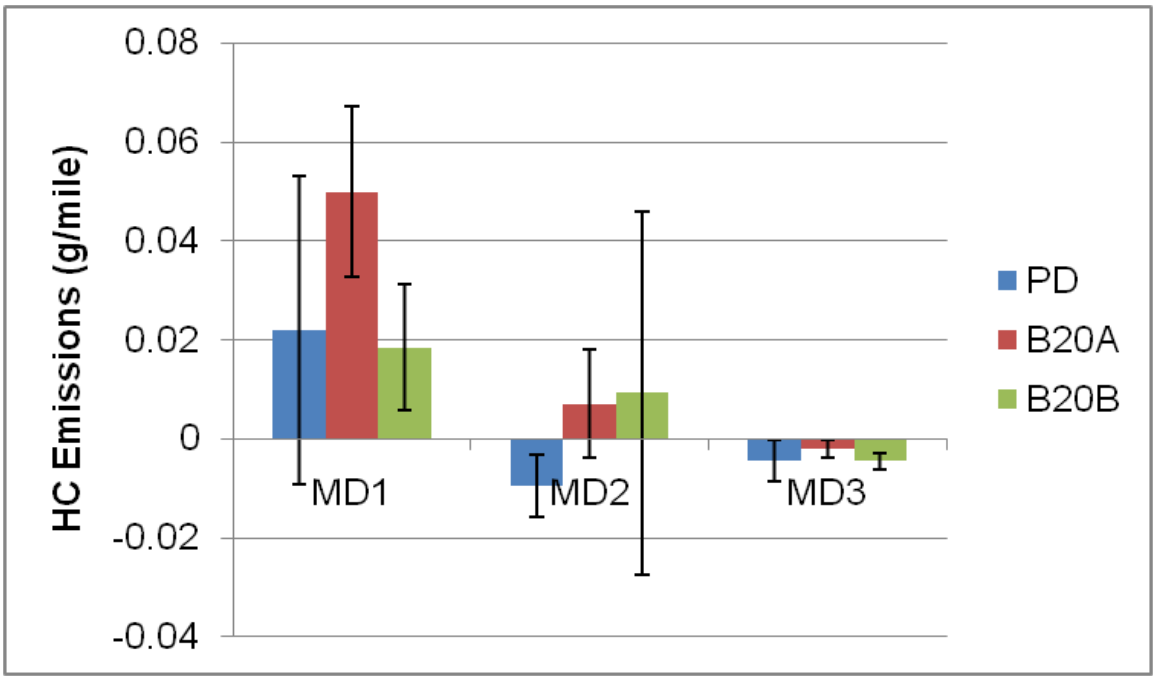

Figure 22: HC emissions comparison for the test fuels.

4.2.5. NO_x Emissions

Figure 23 shows the NO_x emissions from this study. Except for B20B, NO_x emissions at MD2, the biodiesel blends produced slightly higher NO_x emissions than the PD but these variations are statistically insignificant at 95% confidence

level for MD1 and MD2. MD3 data analysis showed that statistically significant differences in emissions started to manifest between the PD and the biodiesel blends. These results are consistent with the findings of many investigators that biodiesel produces slightly higher NO_x emissions than PD. Engine NO_x emissions relationship with vehicle power depends on the units in which they are reported. For instance, brake specific NO_x emissions in g/bhp-hr increase with power while distance specific NO_x emissions reported in g/mile may decrease with vehicle power. This explains the observation in Figure 23, where NO_x emissions (in g/mile) for MD1 and MD2 are much higher than that of MD3. This is in agreement with the findings of Durbin et al. [88] for a 2005 heavy duty truck where distance specific NO_x emissions reported in g/mile were lower at 70 mph compared to 65 mph on I-5 Freeway using cruise control.

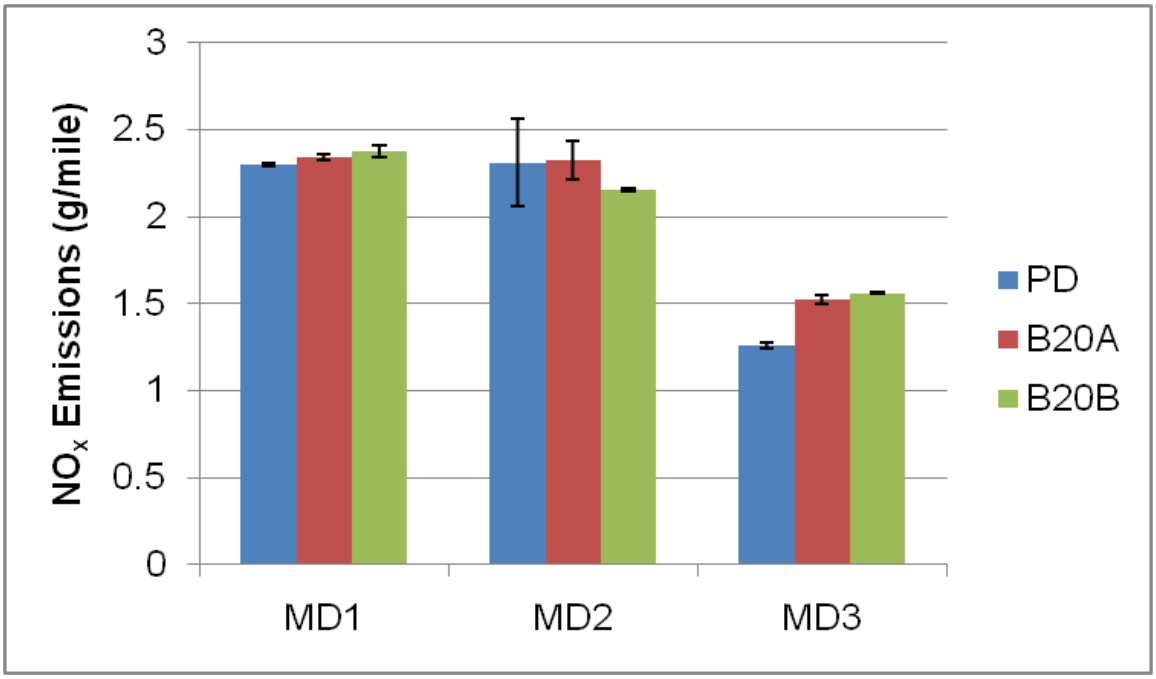

Figure 23: NO_x emissions comparison for the test fuels.

Moreover, NO_x emissions from this study were compared to NO_x emissions obtained from emission factor (EMFAC, 2007 version) modeling tool developed by CARB [89-91]. Base Emission Rates (BER) were estimated from EMFAC tool for the Los Angeles district for this comparison. The NO_x speed correction factor was

applied to the BER to obtain estimates for NO_x emissions for PD fuel only. For the model implementation, ambient temperature of 20^{o}C and relative humidity of 75% were assumed. The month of testing used in the model was November for calendar year 2009 and the NO_x speed correction factors used for correction were obtained from Figure 40 in the appendix. Figure 24 shows the comparison between the NO_x emissions from this study with those obtained from EMFAC. The EMFAC results corroborated the fact that lower NO_x emissions in units of g/mile were produced at high speed compared to low speed as observed in this study. For MD2, B20B produced lower but statistically insignificant NO_x emissions (Figure 23). This may be due to the fact that a higher EGR rate was employed by the engine during testing. If this was the case, then higher EGR rates should translate to higher PM emissions. However, Figure 25 shows that this was masked by the fact that most or part of the PM emissions from B20B at MD2 were oxidized in the DPF. The DPF operation depends on many factors including engine backpressure, exhaust temperature, DPF loading and regeneration rate, and substrate oxidation rate [92].

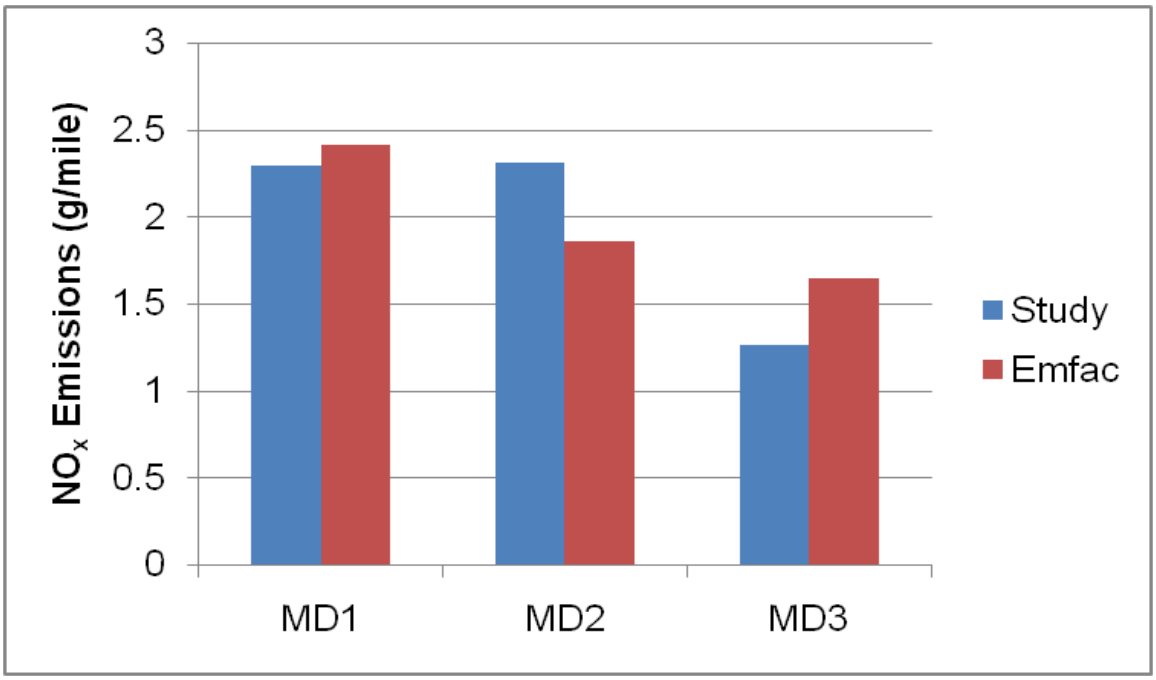

Figure 24: NO_x emissions comparison between this study and EMFAC for PD.

4.2.6. PM Emissions

Figure 25 shows the gravimetric PM emissions obtained from the tests. The figure also shows that there is no distinct pattern for the PM emissions. The error bar on PD plot (three repeat runs) shows the level of variability that could be seen in quantifying low PM mass emissions from DPF equipped vehicles. The lack of definite pattern observed in the figure is due mainly to the operating states of the DPF during each of the test runs which depend on the control strategy of the emissions control system. The emissions from the 2007 truck are generally lower when compared to older trucks. For instance, PM emissions for MD2 from this study are much lower than those obtained in the E-55/59 report for medium heavy duty diesel truck using the MHDDT cruise mode driving schedule. While the emissions for the 2007 truck is of the order of 0.003 g/mile for PD, the E-55/59 reported PM emissions between 0.4 g/mile to 0.8 g/mile for 1999-2002 model year truck (Figure 41 of the E-55/59 final report). This is obviously due to soot oxidation in the DPF, which may mask the effects of other factors such as the fuel. Consequently, it may be difficult to infer the fuel effects on PM emissions without a high count of repeat tests or very long tests to provide high DPF loading.

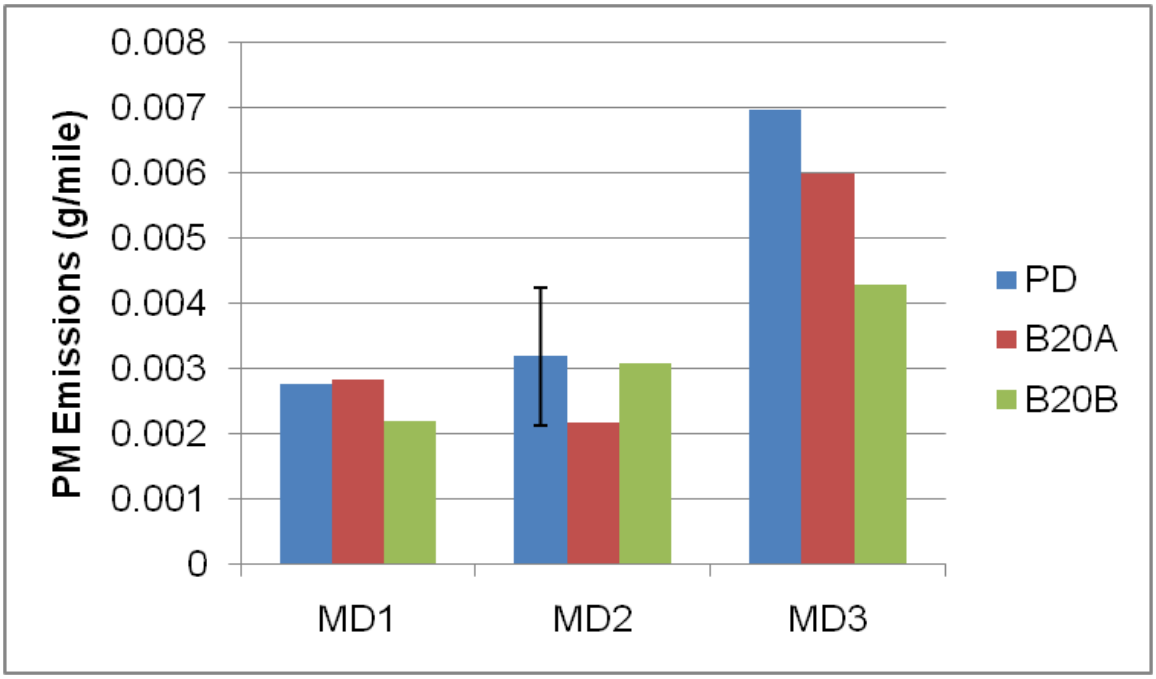

Figure 25: PM emissions comparison for the test fuels.

4.3. Particle Emissions Results

The particle count data collected by DMS500 that are analyzed and reported were low in magnitude especially at MD1 and MD2. This is because of the low vehicle speed operations and the fact that the vehicle was DPF equipped. The low vehicle speed operations (MD1 and MD2) mean that the vehicle operated in light to medium load conditions. Because of the low level of magnitude of particle count data recorded at low speed operations, it is possible that some of the collected data may have been affected by the level of the electrical noise of the DMS 500 equipment (usually below 10^4 dN/dlogDp/cc). Other factors that could impact the results include dilution ratio, dilution temperature, injection pressure, fuel composition, relative humidity, EGR composition and the residence time. In the paragraphs that follow, exhaust particles data were analyzed and compared in terms of particle number concentration, particle GMD, particle mass concentration for each of the drive cycles. This is necessary to show any observable differences that may help explain fuel effects on exhaust particle emissions.

It is also important to show how particle emissions varied with time during testing. The continuous particle emissions data were integrated over the whole size range for each time to estimate the total number of particles emitted at a given time. The total particle number was plotted against time to show how particle emissions varied with time. Figures 37, 38 and 39 of the appendix show the plots for MD1, MD2 and MD3, respectively with outlier points removed. Some of the plots show that particle emissions were nearly constant with time (MD1 and MD2) while others increased over time (MD3). This trend suggest that particle dynamics is highly non linear. It depends on many other factors such as dilution conditions, lubricant effects, and DPF conditions that could explain the trends noticed in the figures.

4.3.1. Lognormal Distribution of Exhaust Particles

4.3.1.1. Particle Size and Number Distributions of PD for MD1, MD2 and MD3

Graphical comparison was made among the data collected for PD for the three drive modes. Figure 26 below shows a bi-modal particle size distribution with most number of particles recorded at MD3, followed by MD2 and MD3, respectively. MD3 requires most power for propulsion which means that most fuel will be consumed. Since more fuel is burned in the engine cylinder, more particles will be formed as a result of longer diffusion combustion duration. It is expected that more volatile particles, which serve as precursors for NMPs, and more carbonaceous agglomerates, which lead to more AMPs, will be produced. Similar argument holds for MD2 and MD1. Figure 26 is representative of the distribution patterns observed for B20A and B20B. Hence, charts for B20A and B20B are not shown.

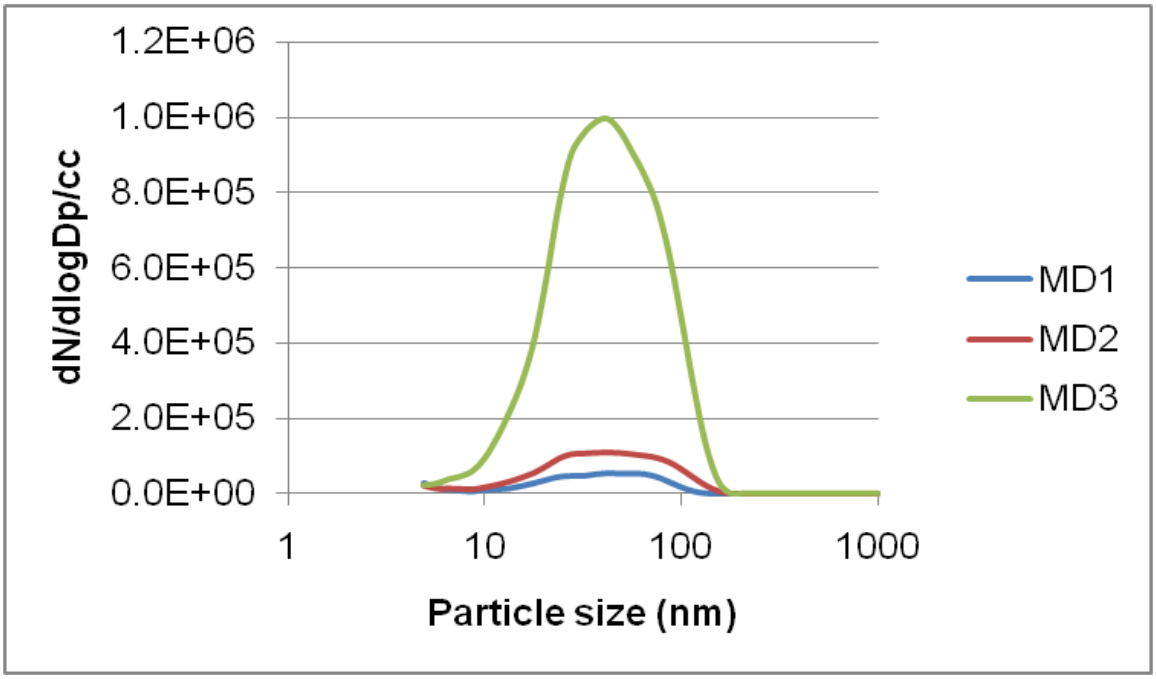

Figure 26: Particle size and number comparison for PD for all drive cycles.

4.3.1.2. Particle Size and Number Distribution for the Test Fuels for MD1

Figure 27 shows a lognormal distribution for the test fuels for MD1. The figure further reveals that exhaust particles existed in two modes namely NMPs, AMPs. The data for the figure were obtained by averaging the data collected over the test duration for each of the test fuel since it was assumed that testing was done at steady state condition. It is observed that, for any of the test fuel, the particle number is predominantly dominated by the NMPs. This is more evident from Figure 30, which shows the number contribution of each of the particle modes for each of the drive cycles. It is also observed, from Figure 27, that PD produced higher number of particles than B20A and B20B. Many factors could contribute to this observation. First, the sulfur and phosphorous contents of lubrication oil that could have entered the combustion chamber affected exhaust particle number emissions in the NMP range. It has been shown by Andersson et al. [46] that sulfur and phosphorous contents of the lubricant that escaped into the chamber lead to higher number of exhaust particles emitted in the NMP range. The sulfur content of the test fuels have little or no effects on nanoparticles emissions because of the

very low sulfur concentrations (between 1-2 ppm concentrations) of the fuels. During dilution and cooling of hot exhaust, heterogeneous nucleation of sulfuric acid and water takes place. This promotes the growth, by deposition, of initial nucleated particle of about 1 nm during condensation and thus leading to their detection by the particle measuring instrument [53]. Second, the fuel injection pressure may have affected the number of particles produced especially for the AMPs. Biodiesel fuels possess physical properties that make them to have higher injection pressure than PD. It does seem that the higher injection pressure contributed in reducing the NMPs and AMPs produced compared to PD. This observation is in agreement with the conclusions of the Sinha et al. [69] that higher injection pressures lead to lower particle emissions especially for AMPs. Furthermore, the oxygen content of biodiesel fuels also contribute to advanced combustion and better fuel atomization and oxidation in locally rich fuel zones. This helps to further reduce particle emissions especially particle mass concentrations.

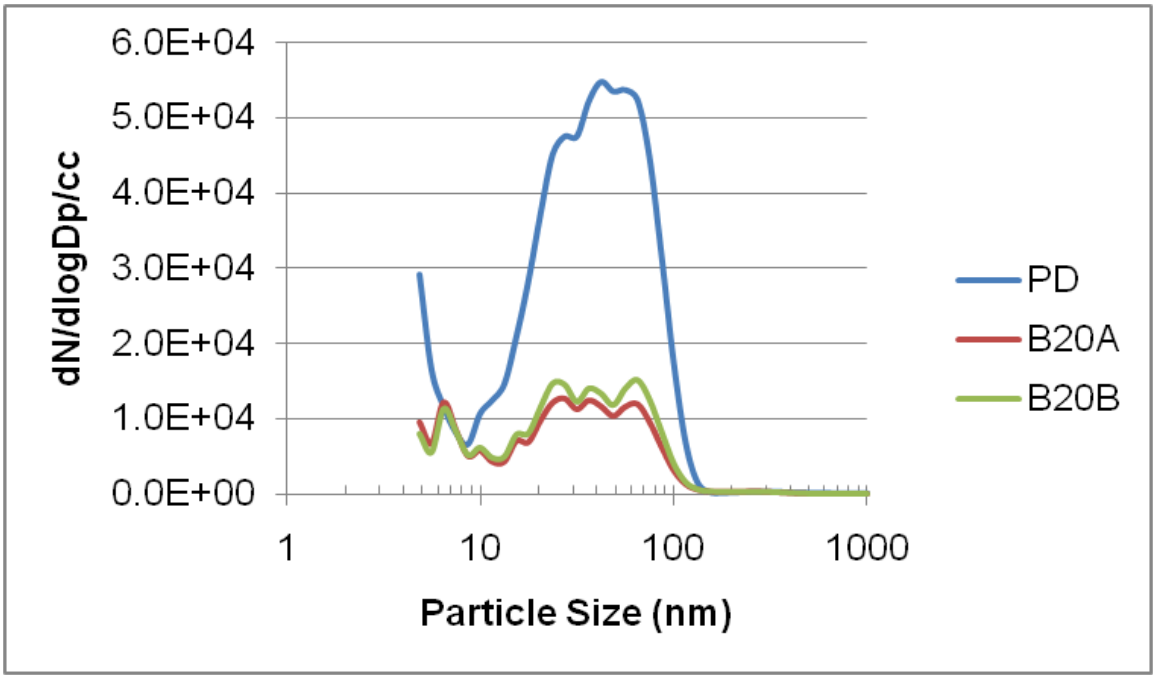

Figure 27: Particle size and number comparison for the test fuels for MD1.

4.3.1.3. Particle Size and Number distribution for the Test Fuels for MD2

Figure 28 shows a lognormal distribution for the test fuels for MD2. Similar to the Figure 27, the exhaust particles also existed in two modes. Two major observations are noticed from the figure. First, it is observed that the particle number concentration levels produced are higher than that of MD1. Figure 30 clearly shows this. Second, it is also observed that B20B produced higher number of particles than PD deviating from the trend observed in Figure 28. The number of exhaust particles produced from B20B (1.76×10^5 particles) is about two times that of PD (9.19×10^4 particles). The ambient conditions seemed to have dominating effects on the particle formation. The PD particle data were an average of three repeat runs done at 25°C, 22°C and 18°C ambient air temperature while the single run B20B data were collected at 15°C. The error bars show the data variability in the three repeat runs for PD. The error bars indicate that particle measurement is highly non-linear and highly susceptible to variations as a result of small change in the measuring condition. This also suggests that the relative humidity and dilution temperature would be different for the test runs. The ambient air temperature could be said to be the dilution temperature since exhaust samples were diluted with HEPA filtered air at the entrance of the primary dilution tunnel.

Thus it can be concluded that more particles, especially the NMPs, were produced at lower ambient temperature (dilution temperature) and higher relative humidity and vice versa. This conclusion is in line with the findings of Abdul-Khalek et al. [53] that dilution temperature and relative humidity affect exhaust particle formation during dilution and cooling processes. Factors such as the DPF action (e.g. loading over time and subsequent regeneration) together with the magnitude of the exhaust temperature and composition of the exhaust gas re-circulated back to the engine (EGR) may have also played a part in this.

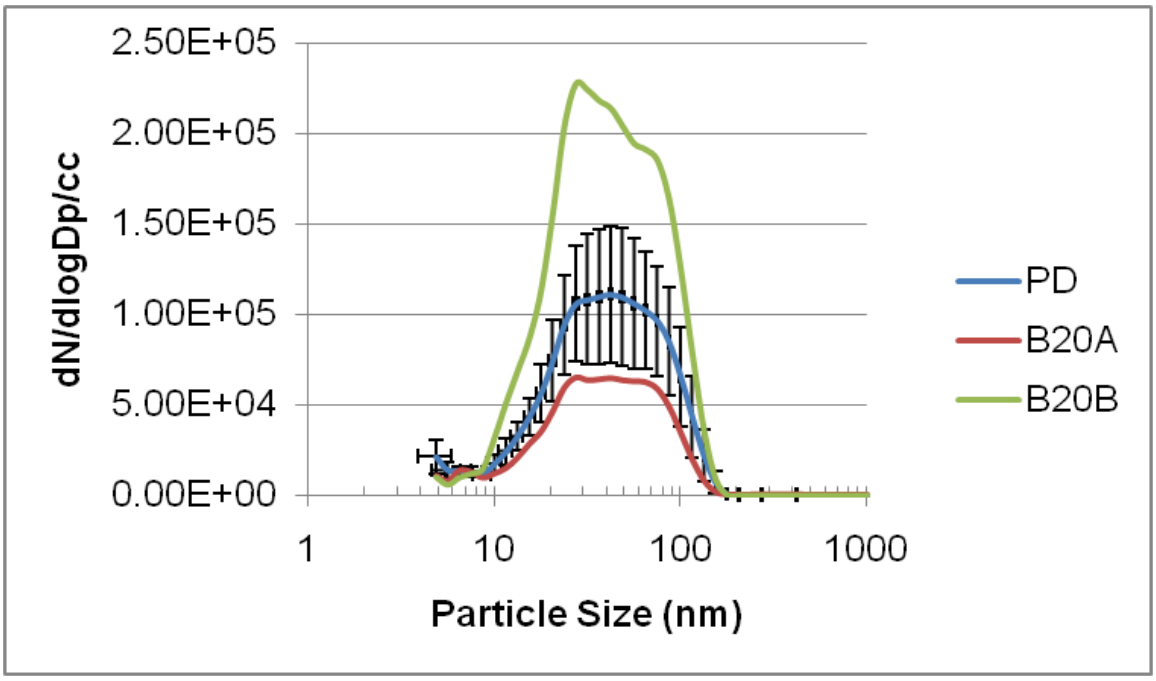

Figure 28: Particle size and number comparison for the test fuels for MD2.

4.3.1.4. Particle Size and Number Distribution for the Test Fuels for MD3

From Figure 29 below, it can be seen that two distinct particle forms were present in the vehicle exhaust similar to that of MD1 and MD2. For MD3, most particles were produced mainly because more fuel was consumed compared to MD1 and MD2. PD produced more exhaust particles than B20A and B20B possibly because the lubricant effect entering the combustion chamber during testing. Between B20A and B20B, many factors could have impacted B20A to produce more particles than B20B. For instance, a report [56] showed that, although the DPF is very effective in removing diesel PM, it produces more quantities of NMPs which increase in quantity as a function of exhaust temperature. In this case, the exhaust temperature data for B20A was slightly higher than that of B20B and this would favor more particles to be produced for B20A. Even at the same flow rate, if the re-circulated exhaust gas (EGR) composition contained more volatile compounds (sulfates), formation of more exhaust particles in the NMP range will be favored.

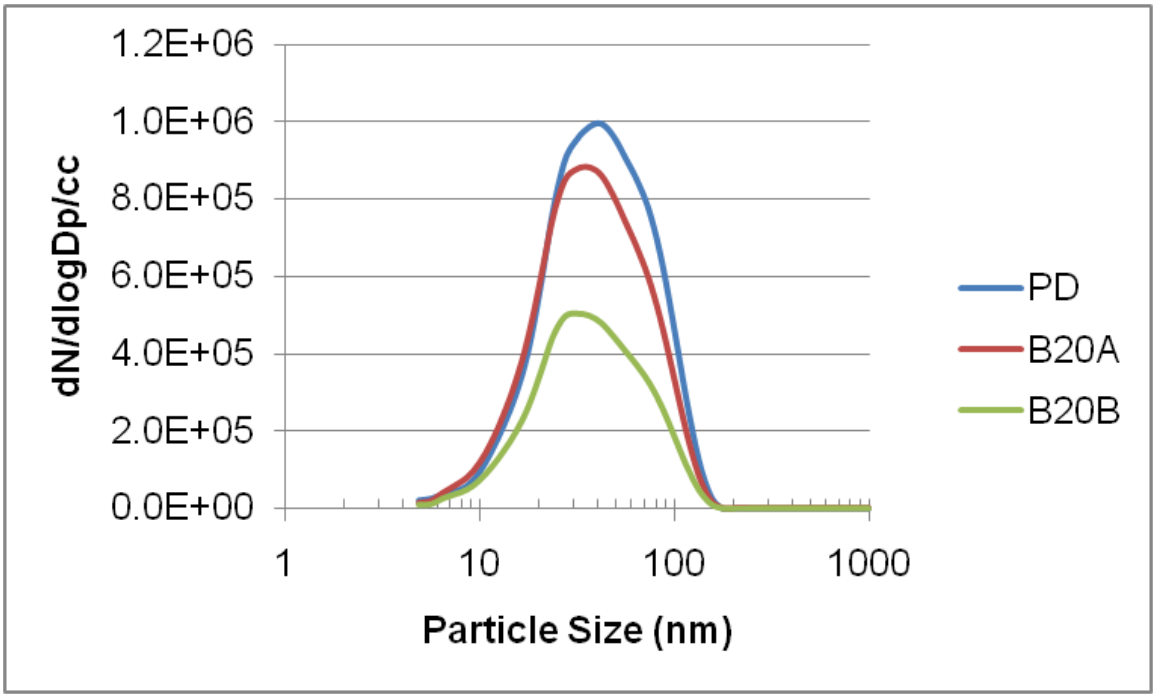

Figure 29: Particle size and number comparison for the test fuels for MD3.

4.3.2. Comparison of Particle Number Concentration for the Test Fuels

Figure 30 shows the comparison of absolute values of number concentrations for each particle modes for the three driving cycles. It can be observed that MD3 produced highest number of particles followed by MD2 and MD1 respectively. This is expected as highest power was required and most fuel was consumed at MD3 thereby producing most exhaust particles. Similarly, MD2 required more power and fuel than MD1 but less power and fuel than MD3 producing more particles than MD1 but less particles than MD3. Another observation is that the particle number comparison is dominated by NMPs for the three fuels under the three driving conditions. This corroborates the fact that exhaust particle number distribution is mainly dominated by NMPs if present. This is especially true for DPF-equipped vehicles. The dominance of exhaust particles number concentration by NMPs is clearly seen in Figure 31. Figure 31 shows that for all the driving modes, the proportion of exhaust particles for each of the particle modes is 60-73% for NMPs and 33-40% for AMPs. In addition, analysis of the all

exhaust particles data for GMD, based on bin widths, reveals the following: For MD1, the GMD for the three fuels ranges between 17.8-22.8 nm for NMPs and 71-73.8 nm for AMPs. For MD2, the GMD for the three fuels ranges between 23.8-26 nm for NMPs and 74.7-76.3 nm for AMPs. Also, for MD3, the GMD for the three fuels ranges between 25.8-27.3 nm for NMPs and 73.1-74.2 nm for AMPs. Thus, it can be inferred that not only does the increase in vehicle power leads to increase in the number of particles emitted for the three fuels; it also increases the size of the particle modes except for AMPs for MD3.

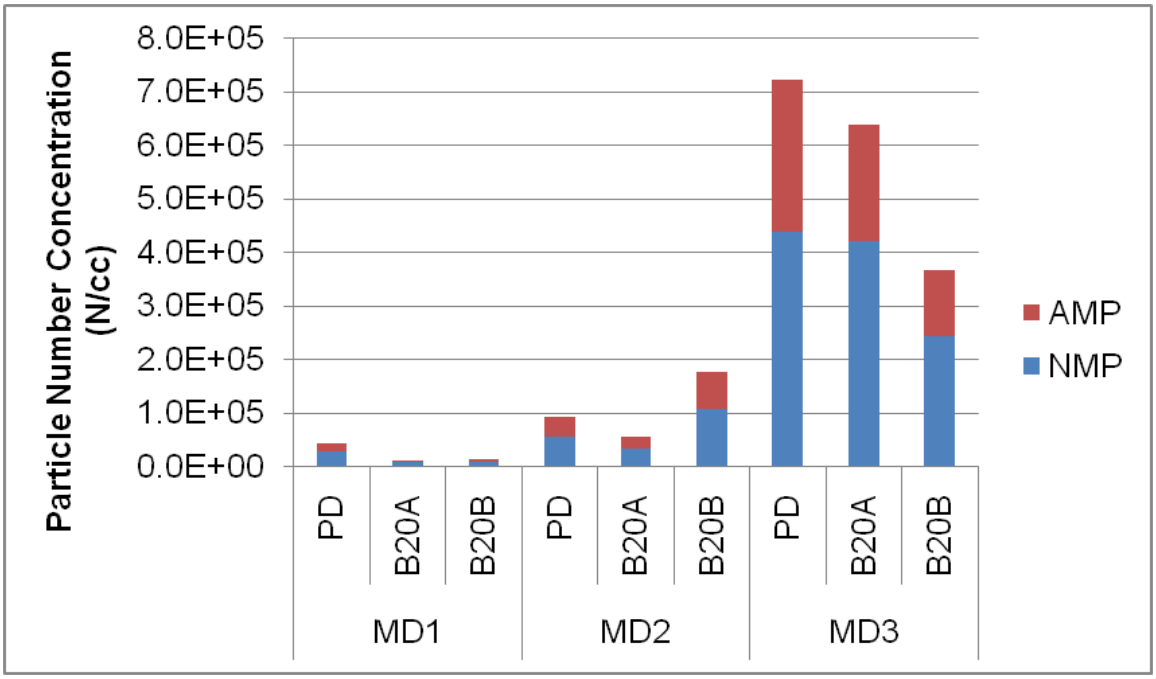

Figure 30: Particle number concentration comparison for the test fuels.

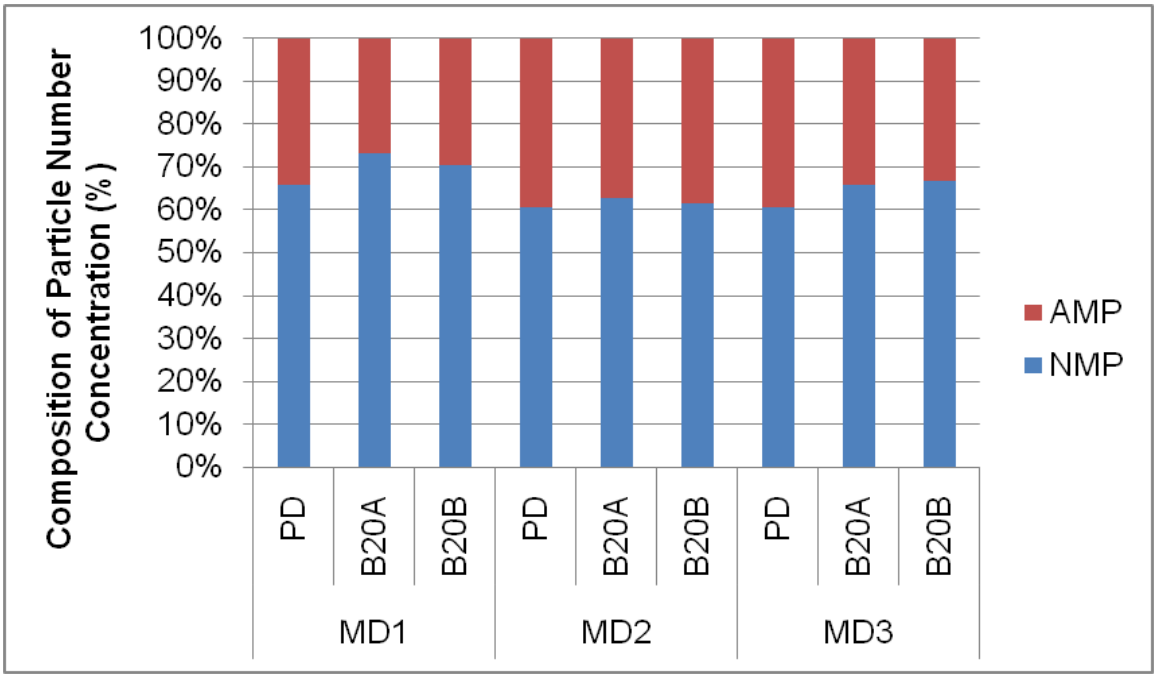

Figure 31: Percentage particle number composition for the test fuels.

4.3.3. Comparison of GMD for the Three Test Fuels

In addition to estimating the GMD for each exhaust particle mode for each of the test runs, the overall GMD combining all the GMD for each of the particle modes was also obtained. Figure 32 displays the overall GMD for each of the test runs with geometric standard deviation of diameter used for the error bars. The figure shows that, for each of the driving mode, the GMD for PD is greater than that of B20A and B20B except for B20B at MD2. It is possible to obtain the GMD value at B20B for MD2 considering the fact that other factors such as ambient conditions (temperature and humidity), EGR fraction components, DPF action that are not fuel related strongly affect exhaust particle formation. The GMD trend observed for PD over the biodiesel blends is expected considering the fact that biodiesel normally has higher oxygen and lower carbon content than PD. Biodiesel physical properties create a higher fuel injection pressure than PD. These biodiesel fuel characteristics lead to advanced and more complete combustion and better fuel oxidation thus producing lower carbon soot than PD. In addition, the sulfur and phosphorous contents of the lubrication oil could have promoted higher

number of particle formation especially in the NMP range.

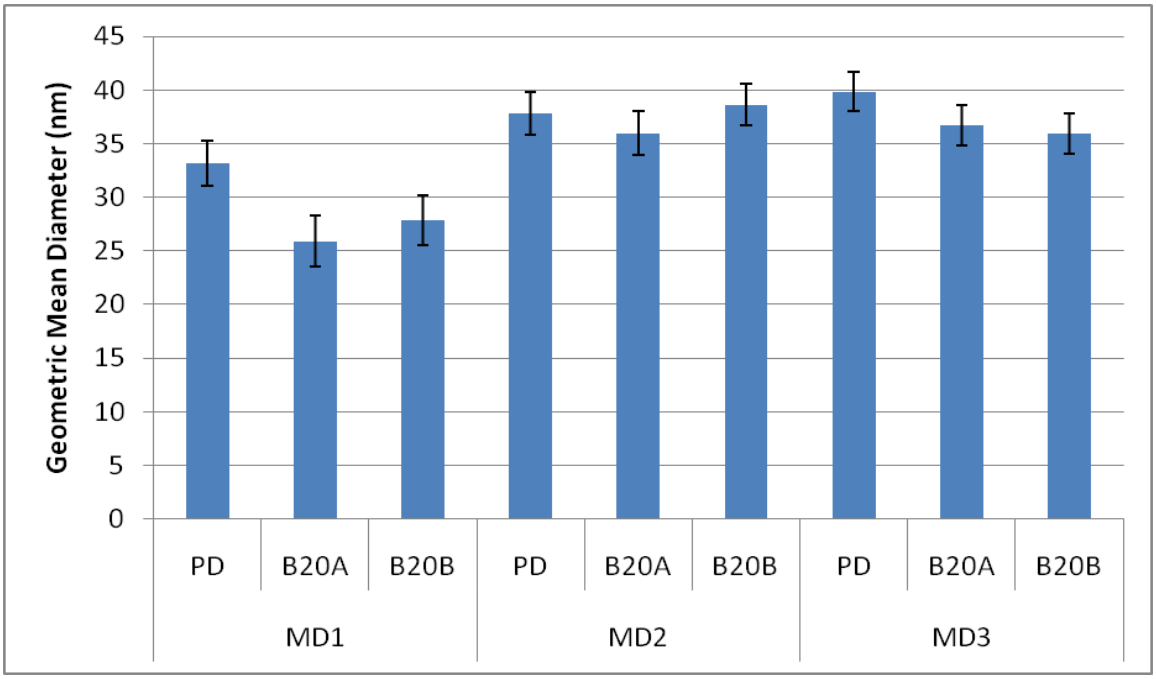

Figure 32: GMD of exhaust particles for the test fuels.

4.3.4. Comparison of Particle Mass Concentration for the Test Fuels

Based on the dilution tunnel's particle size and number distribution data (Figures 27, 28 and 29), exhaust particles' mass in the units of g/mile was estimated using Equation 2 developed by Symonds et al. [83]. The results obtained were compared with the gravimetric PM mass measurement results shown in Figure 25. Figure 33 shows the graphical comparison of exhaust particles' mass (DMS500) with that gravimetric PM mass measurement (Filter) for all the test fuels and the drive modes. This comparison is appropriate to see any similarities or differences since both measurements tend to quantify the magnitude of mass of the particulates emitted by the diesel engine. The PD plots of MD2 are average from three repeat runs while others are plots from single test run. As noted earlier, the PD error bars for MD2 depict the level of variability that may be seen when measuring low PM mass emissions of DPF equipped vehicle. However, one important observation is that the figure shows similar patterns for both measurements. In general, the order of magnitude of mass measurement for

a given cycle is similar. The differences noticed in both measurements, for a given cycle, are probably due to the accuracy of measurement problems associated with low mass filter weighing and also the error inherent in the use of the empirical equation to estimate particle mass from the DMS data.

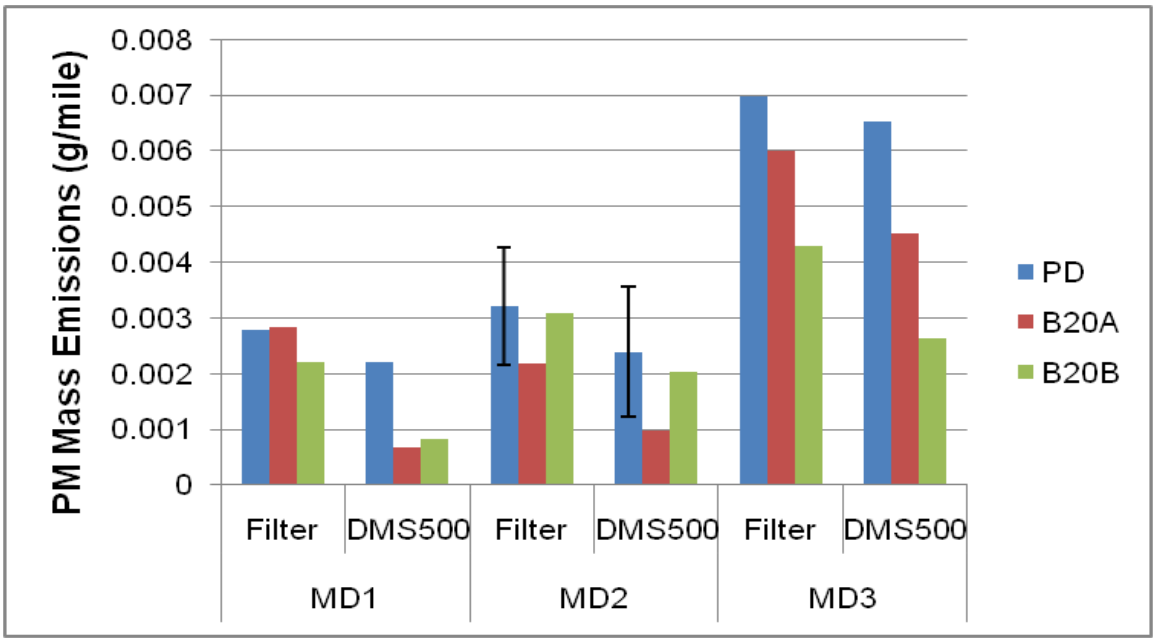

Figure 33: PM mass emissions measurement comparison for the test fuels.

4.3.5. Particle Mass Composition for the Test Fuels

Figure 33 above was further analyzed to determine the components of the mass concentration for the test fuels for the three drive modes. Figure 34, which shows the results of the analysis, reveals that AMPs dominate the exhaust particle mass and the magnitude increases with power consumption. This is expected and is in line with the conclusions of many authors that AMPs dominate the mass concentration while NMPs dominate the number concentration of exhaust particles of a vehicle. The reason for this is that the mass contribution of a particle is proportional to $D^{3.19}$, according to Eqn.1, where D is the particle diameter. Since the size of the AMPs is much bigger than that of NMPs, it is logical that AMPs will contribute more to the mass concentration considering the index of 3.19 even though NMPs contribute more to the number concentration. The mass contribution

of each of the particle modes is more clearly shown in Figure 35. For all the driving modes, the NMPs contribute about 2-8% while the AMPs contribute as high as 98% to the mass concentration. To obtain Figures 34 and 35, the particle size ranges were categorized such that the NMPs range between 5-50 nm while the AMPs range from 50-1000 nm.

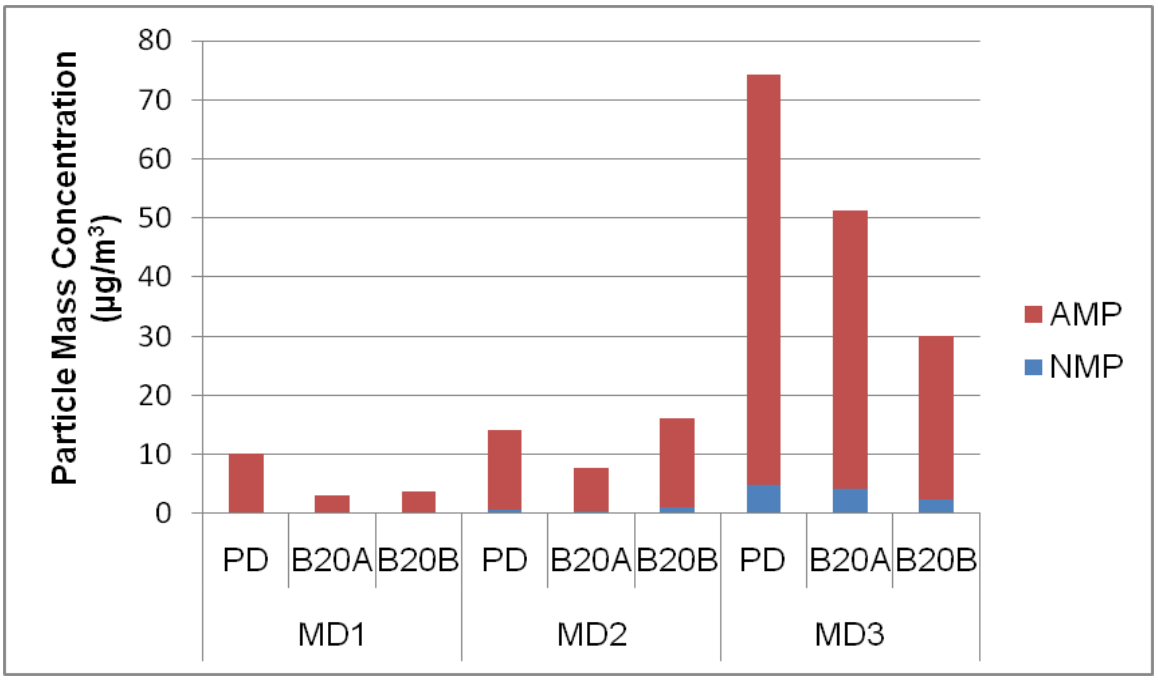

Figure 34: Particle mass composition for the test fuels.

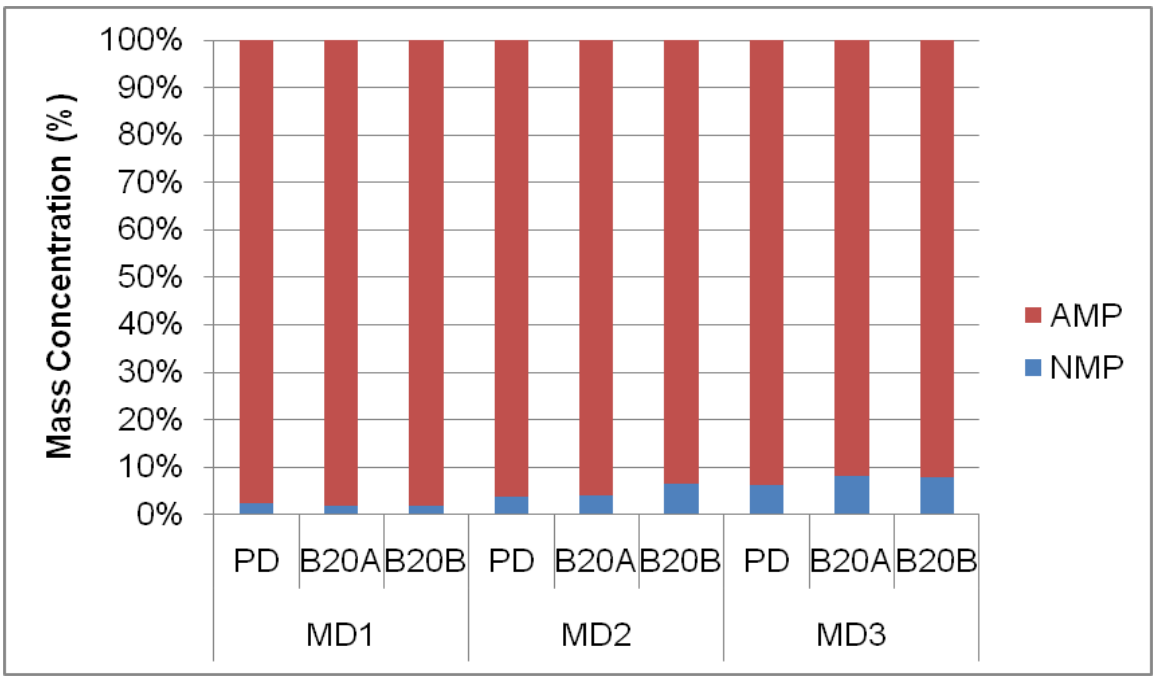

Figure 35: Particle mass concentration for the test fuels.

5. Conclusions and Recommendations

5.1. Conclusions

Two biodiesel blend fuels (B20A and B20B) and PD fuel were tested on a 2007 heavy duty diesel truck equipped with EGR, VTG and DPF under steady state conditions using three drive cycles. Distance-specific regulated emissions, CO_2 emissions, and fuel consumption were quantified. In addition, exhaust particle emissions were also characterized and compared in terms of number, mass and size distributions. The following gives the conclusions drawn from this study.

- Test results for the 20 mph, 35 mph and 50 mph vehicle speeds showed that CO_2 emissions variations among the test fuels are statistically insignificant at 95% confidence level. In addition, the vehicle performance in terms of fuel economy showed that PD had a better fuel economy compared to the biodiesel blends. This is because of higher carbon content in the PD which translates to higher heating value for the fuel.
- The effects of the fuels on CO, HC and PM emissions were difficult to quantify. This is because the other non-fuel effects such as the EGR, the VGT and the DPF effects introduced more complexity into the in-cylinder combustion processes and the formation mechanism.
- The high variability observed in the emissions patterns of CO, HC and PM was dominantly affected by the DPF. Factors which confounded emissions measurement include:
    a) Effects of the DPF loading that changed from time to time.
    b) Effects of changes in EGR and VGT settings as a result of small changes in load or operating conditions.
    c) Effects of changes in ambient conditions during measurement.
- The fuels' effects on NO_x emissions showed that there was an insignificant increases in the biodiesel emissions compared to PD except at the vehicle speed of 35 mph where B20B had lower emissions than the other fuels. This

suggests that the EGR effect also played a significant role on the NO_x emissions pattern observed.

- It is the conclusion of this study that at 0.2 g/bhp-hr NO_x emissions standard, small variations in NO_x emissions due to fuel composition will probably play a small role in the NO_x emissions inventory while older trucks with 2.5 g/bhp-hr and 4 g/bhp-hr emissions standards still continue to operate.
- This study showed that the pattern of exhaust particle emissions observed could not be alluded to fuel effects alone. Other non-fuel factors such as temperature, humidity, EGR fraction composition, DPF loading also played a significant role in exhaust particle composition and emissions.
- The exhaust particle mass concentration distribution chart substantially corroborated the pattern observed from the results of gravimetric PM mass emissions measurement.
- For all tests performed, exhaust particle number emissions are dominated by nanoparticles (NMPs) while the particle mass emissions are dominated by AMPs.
- As the vehicle propulsion power increases, the total particle number and mass emissions increase. This study also shows that the GMD of exhaust particles also increase with vehicle propulsion power.

5.2. Recommendations

Based on the results obtained from this study, it is recommended that future research should be conducted with the following focus areas:

- This study only investigated steady state condition up to the vehicle speed of 50 mph. It is therefore suggested that more tests on 2007 model year engines be conducted using different biodiesel blend proportions under the same steady state condition but at vehicle speeds greater that 50 mph. This is to determine the emissions effects of the fuels at very high speeds as it is m,jh nk nn possible, as noted in this study, that marked differences in CO_2 and NO_x emissions may be observed among the fuels.

- It is recommended that more testing on 2007 model year engines and trucks is required to produce more test data which can be used to study the combined effects of EGR, VGT and DPF on engine emissions. Moreover, since transient EGR and VGT management may differ from steady-state engine management strategies, more data are required for transient dynamometer test cycles.
- It is also recommended that the impact of non-fuel effects such as dilution conditions, and ambient conditions be studied on 2007 or later model year truck both on the dynamometer in the laboratory and on the road.

References

1. Mills, N. L., Tornqvist, H., Robinson, S. D., Gonzalez, M., Darnley, K., MacNee, W., Boon, N. A., Donaldson, K., Blomberg, A., Sandstrom, T., and Newby, D, E., "Diesel Exhaust Inhalation Causes Vascular Dysfunction and Impaired Endogenous Fibrinolysis," *Circulation,* **112**:3930-3936, 2005.
2. Peretz, A., Sullivan, J. H., Leotta, D. F., Trenga. C. A., Sands, F. N., Allen, J., Carlsten, C., Wilkinson, C. W., Gill, E. A., and Kaufman, J. D., "Diesel Exhaust Inhalation Elicits Acute Vasoconstriction in Vivo," *Environ. Health Perspect.,* **116**:937-942, 2008.
3. Tornqvist, H., Mills, N. L., Gonzalez, M., Miller, M. R., Robinson, S. D., Megson, I. L., Macnee, W., Donaldson, K., Soderberg, S., Newby, D. E., Sandstrom, T., and Blomberg, A., "Persistent Endothelial Dysfunction in Humans after Diesel Exhaust Inhalation," *Am. J. Respir. Crit. Care Med.,* **176**:395-400, 2007.
4. Pope, C., "Air Pollution and Health-Good News and Bad," *The New England Journal of Medicine,* **351**:1132–1134, 2004.
5. United States Environmental Protection Agency Fact Sheet: Diesel Exhaust in the United States. EPA 420-F-02-022, June 2003. Available online at http://www.epa.gov/otaq/retrofit/documents/420f03022.pdf.
6. Agarwal, A. K., "Biofuels (Alcohols and Biodiesel) Applications as Fuels for Internal Combustion Engines," *Progress in Energy and Combustion Science,* **33**:233-271, 2007.
7. Tyson, K. S., Bozell, J., Wallace, R., Petersen, E., and Moens, L., "Biomass Oil Analysis: Research Needs and Recommendations," Technical Report by National Renewable Energy Laboratory, Golden, Colorado. NREL/TP-510-34796, June 2004.
8. Hong, H., Wang, M., Bloyd, C., and Putsche, V., "Life-Cycle assessment of Energy Use and Greenhouse Gas Emissions of Soybean-Derived Biodiesel and Renewable Fuels," Environ. Sci. Technol., **43**:750-756, 2009.
9. National Biodiesel Board, "Biodiesel Production," http://www.biodiesel.org/pdf_files/fuelfactsheets/Production.PDF, March, 2010.
10. Engine Manufacturers Association: Technical Statement on the Use of Biodiesel in Compression Ignition Engines. EMADOCS 27902.14, October 2009. Available online at http://www.enginemanufacturers.org/file.asp?F=EMADOCS%2D%2327902%2Dv14%2D2009%5FTechnical%5FStatement%5Fon%5Fthe%5FUse%5Fof%

5FBiodiesel%5FFuel%5Fin%5FCompression%5FIgnition%5FEngines%2Epdf&N=EMADOCS%2D%2327902%2Dv14%2D2009%5FTechnical%5FStatement%5Fon%5Fthe%5FUse%5Fof%5FBiodiesel%5FFuel%5Fin%5FCompression%5FIgnition%5FEngines%2Epdf&C=documents. Accessed on July 29, 2010.

11. Gui, M. M., Lee, K. T., and Bhatia, S., "Feasibility of Edible Oil vs. Non-edible Oil vs. Waste Edible Oil as Biodiesel Feedstock," *Energy,* **33**:1646-1653, 2008.
12. Kansedo J., Lee K. T., and Bhatia S., "Cerbera Odollam (Sea Mango) Oil as a Promising Non-edible Feedstock for Biodiesel Production," *Fuel,* **88**:1148-1150, 2009.
13. Yusuf, C., "Biodiesel from Microalgea," *Biotechnology Advances,* **25**:294-306, 2007.
14. Basha, S. A., Gopal, K. R., and Jebaraj, S., "A Review on Biodiesel Production, Combustion, Emissions and Performance," *Renewable and Sustainable Energy Reviews,* **13**:1628-1634, 2009.
15. Leung, D. Y. C., Wu, X., and Leung, M. K. H., "A Review on Biodiesel Production Using Catalyzed Transesterification," *Applied Energy,* **87**:1083-1095, 2010.
16. Illinois Sustainable Technology Center (ISCT): Feasibility Report-Small Scale Biodiesel Production, Waste Management and Research Center, 2006. Available online at http://www.istc.illinois.edu/tech/small-scale-biodiesel.pdf.
17. Wen, G. D., Xu, Y. P., Ma, H. J., Xu, Z. S., and Tian, Z. J., "Production of Hydrogen by Aqueous-phase Reforming of Glycerol," *Int. J. Hydrogen Energy,* **33**:6657-6666, 2008.
18. Da Silva, G. P., Mack, M., and Contiero, J., "Glycerol:A Promising and Abundant Carbon Source for Industrial Microbiology," *Biotechnology Advances,* **27**:30-39, 2009.
19. Wang, Z., Zhuge, J., Fang, H., and Prior, B. A., "Glycerol Production by Microbial Fermentation: A Review," *Biotechnology Advances,* **19**:201-223, 2001.
20. Graboski, M. S., McCormick, R.L., Alleman, T. L., and Herring, A. M., "The Effect of Biodiesel Composition on Engine Emissions from a DDC Series 60 Diesel Engine," National Renewable Energy Laboratory, Final Report #2, NREL/SR-510-31461, February, 2003. Available online at http://www.biodiesel.org/resources/reportsdatabase/reports/gen/20030201_gen-361.pdf.
21. United States Environmental Protection Agency: A Comprehensive Analysis of Biodiesel Impacts on Exhaust Emissions, Draft Technical Report, EPA420-P-02-001, 2002.

22. Wang, W. G., Lyons, D. W., Clark, N. N., and Gautam, M., “Emissions from Nine Heavy Trucks Fueled by Diesel and Biodiesel Blend without Engine Modification,” *Environ. Sci. Technol.,* **34**:933 – 939, 2000.

23. Lin, B., Haung, J., and Haung, D., “Experimental Study of the Effects of Vegetable Oil Methyl Ester on Diesel Engine Performance Characteristics and Pollutant Emissions,” *Fuel,* **88**:1779 – 1785, 2009.

24. Nabi, N., Rahman, M., and Akhter, S., “Biodiesel from Cotton Seed Oil and its Effects on Performance and Exhaust Emissions,” *Applied Thermal Engineering,* **29**:2265 – 2270, 2009.

25. Muzumdar, B. and Agarwal, A. K., “Performance, Emissions and Combustion Characteristics of Biodiesel (Waste Cooking Oil Methyl Ester) Fueled IDI Diesel Engine,” SAE Technical Paper 2008-01-1384, 2008.

26. Raheman, H. and Phadatare, A. G., “Diesel Engine Emissions and Performance from Karanja Methyl Ester and Diesel,” *Biomass and Bioenergy,* **27**:393 - 397, 2004.

27. McCormick, R. L., Tennant, C. J., Hayes, R. R., Black, S., Ireland, J., McDaniel, T., Williams, A., and Frailey, M., “ Regulated Emissions from Biodiesel Tested in Heavy – Duty Engines Meeting 2004 Emission Standards,” SAE Technical Paper 2005-01-2200, 2005.

28. Nine, R. D., Clark, N. N., Mace, B. E., Morrison, R. W., Lowe, P. C., Remcho, V. T., and Mclaughlin, L.W., “Use of Soy–Derived Fuel for Environmental Impact Reduction in Marine Engine Applications,” *American Society of Agricultural Engineers,* **43**(6): 1383 – 1391, 2000.

29. McCormick, R.L., Ross, J. D., and Graboski, M. S., “Effect of Several Oxygenates on Regulated Emissions from Heavy-Duty Diesel Engines,” *Environ. Sci.Technol.,* **31**(4):1144 - 1150, 1997.

30. Nuszkowski, J., Thompson G. J., Tincher, R., and Clark, N. N., “Heat Release and Emissions Characteristics of B20 Biodiesel Fuels during Steady State and Transient Operation,” SAE Technical Paper 2008-01-1377, 2008.

31. Thompson, G. J. and Nuszkowski, J., “Neat Fuel Influence on Biodiesel Blend Emissions,” *Engine Research,* **11**(1): 61 – 77, 2009. DOI: 10.1243/14680874JER04909.

32. Sheehan, J., Camobreco, V., Duffield, J., Graboski, M., and Shapouri, H., “An Overview of Biodiesel and Petroleum Diesel Life Cycles,” National Renewable Energy Laboratory, NREL/TP-580-24772, May 1998.

33. United States Environmental Protection Agency: Alternative Control Techniques Document-NOx Emissions from Stationary Gas Turbines. EPA-453/R-93-007, January 1993. Available online at http://www.epa.gov/ttncatc1/dir1/gasturb.pdf.

34. Mueller, C. J., Boehman, A. L., and Martin, G. C., “An Experimental Investigation of the Origin of Increased NOx Emissions When Fueling a Heavy – Duty Compression – Ignition Engine with Soy Biodiesel,” SAE Technical Paper 2009-01-1792, 2009.

35. Lapuerta, M., Armas, O., and Rodriguez–Fernandez, J., “Effects of Degree of Unsaturation of Biodiesel Fuels on NOx and Particulate Emissions,” SAE Technical Paper 2008-01-1676, 2008.

36. Miller, W. R., Klein, J. T., Mueller, R., Doelling, W., and Zuerbig, J., “The Development of Urea-SCR Technology for US Heavy Duty Trucks,” SAE Technical Paper 2000-01-0190, 2000.

37. Tsolakis, A., Megaritis, A., Wyszynski, M. L., and Theinnoi, K., “Engine Performance and Emissions of a Diesel Engine Operating on Diesel-RME (Rapaseed Methly Ester) Blends with EGR (Exhaust Gas Recirculation),” *Energy,* **32**:2072-2080, 2007.

38. Rajan, K. and Senthil Kumar, K. R., “The Effect of Exhaust Gas Recirculation (EGR) on the Performance and Emission Characteristics of Diesel Engines with Sunflower Oil Methyl Esther,” *Chemical Engineering Research,* **1**(1): 31 – 39, 2009.

39. Verbeek, R., Aken, M., and Verkiel, M., “DAF Euro-4 Heavy Duty Diesel Engine with TNO EGR System and CRT Particulates Filter,” SAE Technical Paper 2001-01-1947, 2001.

40. Hohl, Y. Amstutz, A., Onder, C., and Guzzella, L., “Retrofit Kit to Reduce NO_x and PM Emissions from Diesel Engines Using a Low-Pressure EGR and a DPF System with FBC and Throttling for Active Regeneration Without Production of Secondary Emissions,” SAE Technical Paper 2008-01-0330, 2008.

41. Chatterjee, S., Conway, R., Viswanathan, S., Blomquist, M., Klusener, B., and Andersson, S., “NO_x and PM Control from Heavy Duty Diesel Engines Using a Combination of Low Pressure EGR and Continuously Regenerating Diesel Particulate Filter,” SAE Technical Paper 2003-01-0048, 2003.

42. Ballam, E., “2010 Emissions Standards Limit Apparatus Engine Choices,” http://www.firerescue1.com/fire-products/apparatus-accessories/articles/468238-2010-Emissions-Standards-Limit-Apparatus-Engine-Choices/. March 2009.

43. Khair, M.K., and Jääskeläinen, H. “Emission Formation in Diesel Engines,” <http://dieselnet.com/tech/diesel_emiform.html#pm>.

44. Johnson, J. P., Kittelson, D. B., and Watts, W. F., “Source Apportionment of Diesel and Spark Ignition Exhaust Aerosol Using On-Road Data from the Minneapolis Metropolitan Area,” *Atmospheric Environment,* **39**:2111-2121, 2005.

45. Kittlelson, D. B., “Engines and Nanoparticles: A Review,” *Aerosol Sci.,* **29(5/6)**:575-588, 1998.

46. Andersson, J., Preston H., Warrens C., and Brett, P., “Fuel and Lubricant Effects on Nucleation Mode Particle Emissions From a Euro III Light Duty Diesel Vehicle,” SAE Technical Paper 2004-01-1989, 2004.

47. Farrar-Khan, J. R., Andrews, G. E., Williams, P. T., and Bartle, K. D., “The Influence of Nozzle Sac Volume on the Composition of Diesel Particulate Fuel Derived SOF,” SAE Technical Paper 921649, 1992.

48. Dec, J. E., “A Conceptual Model of DI Diesel Combustion Based on Laser-Sheet Imaging,” SAE Technical Paper 970873, 1997.

49. Ahlvik, P., Ntziachristos, L., Keskinen, J., and Virtanen A., “Realtime Measurements of Diesel Particle Size Distribution with an Electrical Low-Pressure Impactor,” SAE Technical Paper 980410, 1998

50. Heywood, J. B., “Internal Combustion Engine Fundamentals, “McGraw-Hill, New York, ISBN 0-07-100499-8, 1988.

51. Abdul-Khalek, I. S. and Kittleson, D. B., “Real Time Measurement of Volatile and Solid Exhaust Particles Using a Catalytic Stripper,” SAE Technical Paper 950236, 1995.

52. Abdul-Khalek, I. S., Kittleson D. B., Grakow, B. R., Wei, Q., and Brear, F., “Diesel Exhaust Particle Size: Measurement Issues and Trends,” SAE Technical Paper 98P-353, 1998.

53. Abdul-Khalek, I. and Kittleson, D., “The Influence of Dilution Conditions on Diesel Exhaust Particle Size Distribution Measurements,” SAE Technical Paper 1999-01-1142, 1999.

54. GRPE-48-11 (Informal document No.), “Conclusions on Improving Particulate Mass Measurement Procedures and New Particle Number Measurement Procedures Relative to the Requirements of the 05 Series of Amendments to Regulation No.83, Transmitted by the Chairman of the Particle Measurement Programme Group in Conjunction with the Experts from Germany, Sweden, Switzerland and the UK (2004)”.

55. Tsolakis A., “Effects of Particle Size Distribution from the Diesel Engine Operating on RME-Biodiesel with EGR,” *Energy & Fuels,* **20**:1418-1424, 2005.

56. Kittleson, D. B., Watts, W. F., Johnson, J. P., Rowntree, C., Payne, M., Goodier, S., Warrens, C., Preston, H., Zink, U., Ortiz, M., Goersmann, C., Twigg, M. V., Walker, A. P., and Caldow, R., “On-Road Evaluation of Two Diesel Exhaust Aftertreatment Devices,” *Aerosol Sci.,* **37**:1140-1151, 2006.

57. Lee, J., Goto, Y., and Odaka, M., “Measurement of the Diesel Exhaust Particle Reduction Effect and Particle size Distribution in a Transient Cycle

Mode with an Installed Diesel Particulate Filter (DPF)," SAE Technical Paper 2002-01-1005, 2002.

58. Abdul-Khalek, I. S., Kittleson, D. B., and Brear, F., "Diesel Trap Performance: Particle Size Measurements and Trends," SAE Technical Paper 982599, 1998.
59. Mayer, A., Egli, H., Burtscher, H., Czerwinski, J., and Gehrig, H., "Particle Size Distribution Downstream Traps of Different Design," SAE Technical Paper 950373, 1995.
60. Bagley, S. T., Baumgard, K. J., Gratz, L. D., Johnson, J. J., and Leddy, D.G., "Characterization of Fuel and After-Treatment Device Effects on Diesel Emissions," Health Effects Institute, Cambridge, MA, Report 76, 1996. http://healtheffects.org/Pubs/st76.htm.
61. Baumgard, K. J. and Johnson, J. H., "The Effect of Fuel and Engine Design on Diesel Exhaust Particle Size Distributions," SAE Technical Paper 960131, 1996.
62. Donaldson, K., Li, X. Y., and MacNee, W., "Ultrafine (Nanometre) Particle Mediated Lung Injury," *Aerosol Sci.,* **29**:553-560, 1998.
63. United States Environmental Protection Agency: Air Quality Criteria for Particulate Matters. Volume I of II, EPA/600/P-99/002aF, October 2004.
64. Kittleson, D., Johnson, J., Watts, W., Wei, Q., Drayton, M., Paulsen, D., and Bukowiecki, N., "Diesel Aerosol Sampling in the Atmosphere," SAE Technical Paper 2000-01-2212, 2000.
65. Lakkireddy, V. R., Mohammed, H., and Johnson, J. H., "The Effects of a Diesel Oxidation Catalyst and a Catalyzed Particulate Filter on Particle Size Distribution from a Heavy Duty Diesel Engine," SAE Technical Paper 2006-01-0877, 2006.
66. Kittelson, D.B., Watts, W. F., Johnson, J., "Diesel Aerosol Sampling Methodology – CRC E-43: Final Report." University of Minnesota, Report for the Coordinating Research Council, 19 August 2002. http://www.crcao.com/reports/recentstudies00-02/UMN%20Final%20E-43%20Report.pdf.
67. Krahl, J., Munack, A., Schroder, O., Stein, H., and Bunger, J., "Influence of Biodiesel and Different Designed Fuels on the Exhaust Gas Emissions and Health Effects," SAE Technical Paper 2003-01-3199, 2003.
68. Tan, P., Lou, D., and Hu, Z., "Nucleation Mode Particle Emissions from a Diesel Engine with Biodiesel and Petroleum Diesel Fuels," SAE Technical Paper 2010-01-0787, 2010.

69. Sinha, A., Chandrasekharan, J., Nargunde, J., Bryzik, W., Henein, N., and Acharya, K., “Effects of Biodiesel and its Blends on Particulate Emissions from HSDI Diesel Engine,” SAE Technical Paper 2010-01-0798, 2010.

70. Jung, H., Kittelson, D. B., and Zachariah M. R., “Characteristics of SME Biodiesel-Fueled Diesel Particle Emissions and the Kinetics of Oxidation,” *Environ. Sci. Technol.,* **40**:4949-4955, 2006.

71. Kim, H. and Byungchul, C., “The Effect of Biodiesel and Bioethanol blended Diesel Fuel on Nanoparticles and Exhaust Emissions from CRDI Diesel Engine,” *Renewable Energy,* **35**:157-163, 2010.

72. Tindale, M., Price, P., and Chen, R., “The Impact of Biodiesel on Particle Number, Size and Mass Emissions from a Euro 4 Diesel Vehicles,” SAE Technical Paper 2010-01-0796, 2010.

73. Park, S., Kim, H., and Choi, B., “Emissions Characteristics of Exhaust Gases and Nanoparticles from a Diesel Engine with Biodiesel-Diesel Fuel (B20),” *Mechanical Science and Technology,* **23**:2555-2564, 2009.

74. Tan, P., Hu, Z., Lou, D., and Li, B., “Particle Number and Size Distribution from a Diesel Engine with Jatropha Biodiesel Fuel,” SAE Technical Paper 2009-01-2726, 2009.

75. Lapuerta, M., Rodrı´guez-Ferna´ndez, J., Agudelo, J. R., “Diesel Particulate Emissions from Used Cooking Oil Biodiesel,” *Bioresource Technol.,* **99(4)**:731-740, 2008.

76. Bagley, S. T., Gratz, L. D., Johnson, J. H., and McDonald, J. F., “Effects of an Oxidation Catalytic Converter and a Biodiesel Fuel on the Chemical, Mutagenic, and Particle Size Characteristics of Emissions from a Diesel Engine. *Environ. Sci. Technol.,* **32**:1183–1191, 1998.

77. Chen, Y. C., and Wu, C. H., “Emissions of Submicron Particles from a Direct Injection Diesel Engine by Using Biodiesel,” Environ. Sci. Health, **A37** (5):829–843, 2002.

78. Lapuerta, M., Armas, O., and Ballesteros, R., “Diesel Particulate Emissions from Biofuels Derived from Spanish Vegetable Oils,” SAE Technical Paper 2002-01-1657, 2002.

79. Aakko, P., Nylund, N. O., Westerholm, M., Marjamaki, M., Moisio, M., and Hillamo, R., “Emissions from Heavy-Duty Engine with and without Aftertreatment Using Selected Biofuels,” FISITA World Automotive Congress Proceedings, F02E195, 2002.

80. Wu, Y., Carder, D., Shade, B., Atkinson, R., Clark, N., and Gautam, M., “A CFR 1065 – Compliant Transportable/On Road Low Emissions Measurement Laboratory with Dual Primary Full–Flow Dilution Tunnels,” Proceedings of ASME Internal Combustion Engine Division 2009 Spring Technical Conference, ICES2009 – 76090, 2009.

81. "Automotive Emission Analyzer System MEXA-7200 Manual," Horiba, Japan, April, 2007

82. Khalek, I. A., "2007 Diesel Particulate Measurement Research, "CRC Final Report Project E-66-Phase 3," Southwest Research Institute, San Antonio, Texas, 2007.

83. Symunds, J. P. R., Reavell, K. S. J., Olfert, J. S., Campbell, B. W., and Swift, S. J., "Diesel Soot Mass Calculation in Real-Time with a Differential Mobility Spectrometer," *Aerosol Science*, **38**:52-68, 2007.

84. "DMS 500 Fast Particulate Spectrometer User Manual, Version 3.1," Cambustion, United Kingdom, 2010.

85. Stepper, M. R., "Data Link Overview for Heavy Duty Vehicle Applications," SAE Technical Paper 902215, 1990.

86. California Air Resources Board, "Proposed Methodology to Model Carbon Dioxide Emissions and Estimate Fuel Economy," Available online at http://www.arb.ca.gov/msei/onroad/downloads/pubs/co2final.pdf. Accessed October 2010.

87. Clark, N. N., Gautam, M., Wayne, S. W., Lyons, D. W., and Thompson, G., "Heavy-Duty Vehicle Chassis Dynamometer Testing for Emissions Inventory, Air Quality Modeling, Source Apportionment and Air Toxics Emissions Inventory," CRC Report No. E55/59, August 2007.

88. Durbin, T. D., Johnson, K., Miller, J. W., Maldonado, H., and Chernich, D., "Emissions from Heavy-duty Vehicles Under On-road Driving Conditions," *Atmospheric Environment,* **42**:4812-4821, 2008.

89. California Air Resources Board, "EMFAC 2007, Version 2.30 Users Guide," Available online at http://www.arb.ca.gov/msei/onroad/downloads/docs/user_guide_emfac2007.pdf

90. Hancock, B., "On-Road Emissions Inventory Fuel Correction Factors," Technical Memo from California Air Resources Board, July 2005. Available online at http://www.arb.ca.gov/msei/onroad/techmemo/onroad_emissions_invntry_fuel_corr_factors.pdf

91. Zhou, L., "Revision of Heavy Duty Truck Emission factor and Speed correlation Factors," Technical Memo on EMFAC Modeling, October, 2006. Available online at http://www.arb.ca.gov/msei/onroad/techmemo/modification_hhddt_speed_and_speed_corr_factors.pdf

92. Min, J., Lee, C., Kim, H., Jung, H., and Kim, Y., "Development and Performance of Catalytic Diesel Particulate Filter Systems for Heavy-Duty Diesel Vehicles," SAE Technical Paper 2005-01-0664, 2005.

93. Bernemyr, H. and Angstrom, H., “Number Measurements of Diesel Exhaust Particles – Influence of Dilution and Fuel Sulphur Content,” SAE Technical Paper 2007-01-0064, 2007.

Appendix

The following tables below show the laboratory analysis report for B20A and B20B. The analysis was done by Meg Corp Fuel Consulting using ASTM D7467-09A test procedure. Table 8 gives the report for B20A while Table 9 gives report for B20B.

Table 8: Laboratory analysis report for B20A

METHOD	RESULTS	SPECIFICATION
D 287 (API Gravity)	37.1 (Composite)	30.0 minimum
D 86 (Distillation)	406 IBP 438 10% 510 50% 620 90% 646 FBP	650 maximum °F For 90%
D 4737 (Cetane Index)	51.9 Cetane	40 minimum
D 613 (Cetane Number)	51.8 Cetane	40 minimum
D 5453 (Sulfur)	1.0 ppm	15 ppm (ULSD)
D 93 (Flash Point P.M.)	168°F (Composite)	125 °F minimum
D 130 (Corrosion)	1a	No. 1 maximum
D 2500 (Cloud Point)	12°F	Reported
Viscosity (D 445)	2.78 cST	1.9-4.1
D 7371 (Biodiesel Concentration)	20.7%	% Volume
EN 14112 (Oxidation Stability)	6.07 HRS	6 Hours minimum
Water (D 6304 Karl Fischer)	58 ppm	< 100 ppm*
D 2709 (Water and Sediment)	0.00 vol. %	0.05 maximum Vol. %
D 874 (Sulfated ASH)	<0.001%	0.01% maximum
D 524 (Carbon Residue)	0.08%	0.35% maximum
D 664 (Acid Number)	0.06 mg KOH/g	0.30 maximum mg KOH/g
D 6079 (Lubricity HFRR)	234 µm	520 max.imum µm
D 4951 (Phosphorus Content)	<0.001%	0.001% maximum

Table 9: Laboratory analysis report for B20B

METHOD	RESULTS	SPECIFICATION
D 287 (API Gravity)	37.8 (Composite)	30.0 minimum
D 86 (Distillation)	408 IBP 444 10% 510 50% 620 90% 650 FBP	650 maximum. °F For 90%
D 4737 (Cetane Index)	53.7 Cetane	40 minimum
D 613 (Cetane Number)	59.4 Cetane	40 minimum
D 5453 (Sulfur)	1.5 ppm	15 ppm (ULSD)
D 93 (Flash Point P.M.)	170°F (Composite)	125 °F minimum
D 130 (Corrosion)	1a	No. 1 maximum
D 2500 (Cloud Point)	20°F	Reported
Viscosity (D 445)	2.24 cST	1.9-4.1
D 7371 (Biodiesel Concentration)	21.3%	% Volume
EN 14112 (Oxidation Stability)*	3.18 HRS	6 Hours minimum
Water (D 6304 Karl Fischer)	70 ppm	< 100 ppm*
D 2709 (Water and Sediment)	0.00 vol. %	0.05 maximum Vol. %
D 874 (Sulfated ASH)	<0.001%	0.01% maximum
D 524 (Carbon Residue)	0.05%	0.35% maximum
D 664 (Acid Number)	0.12 mg KOH/g	0.30 maximum mg KOH/g
D 6079 (Lubricity HFRR)	249 µm	520 maximum µm
D 4951 (Phosphorus Content)	<0.001%	0.001% maximum

*Does not meet specification.

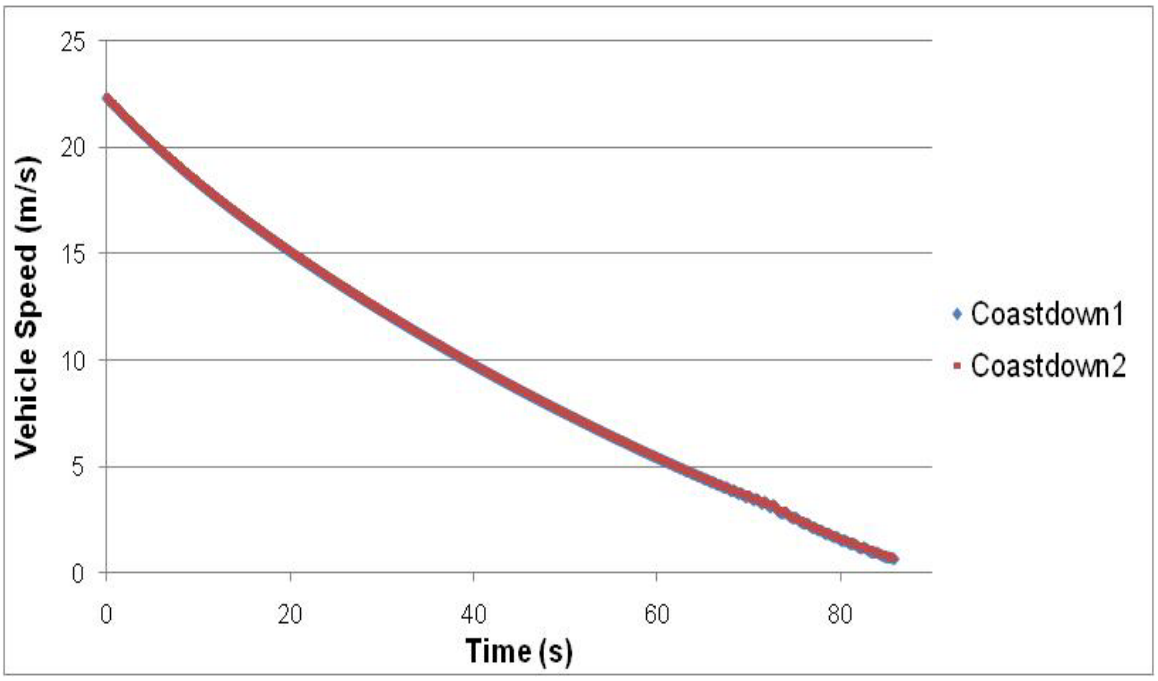

Figure 36: Vehicle speed versus time (coast down data).

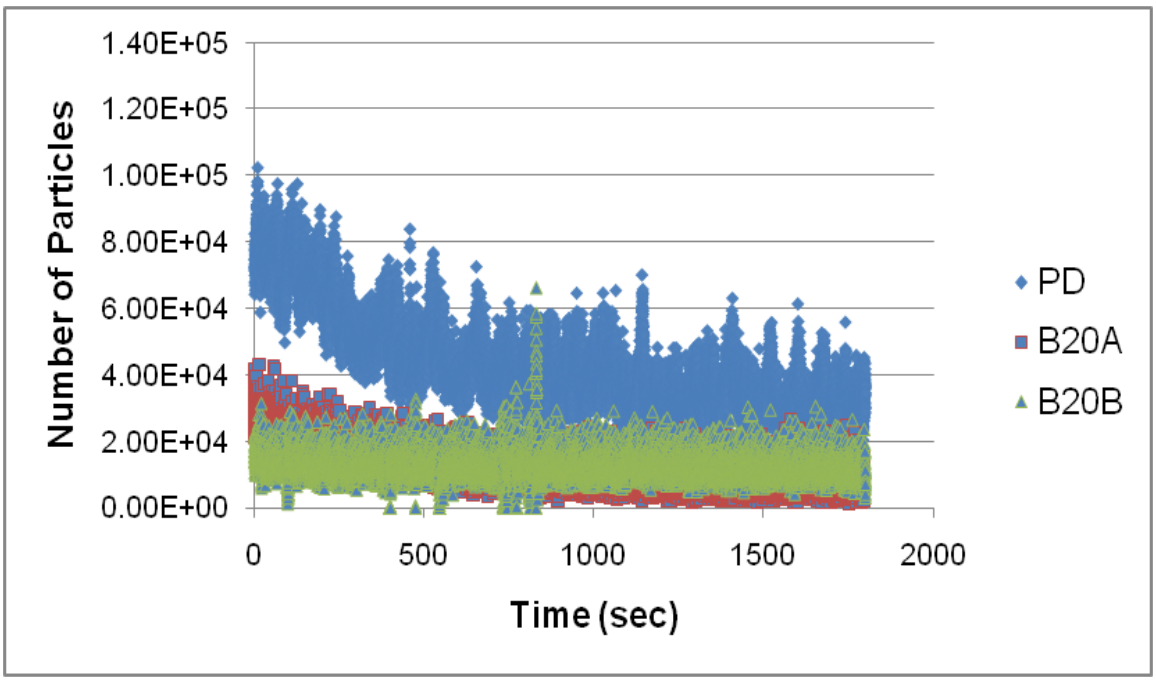

Figure 37: Particle emissions versus time for MD1.

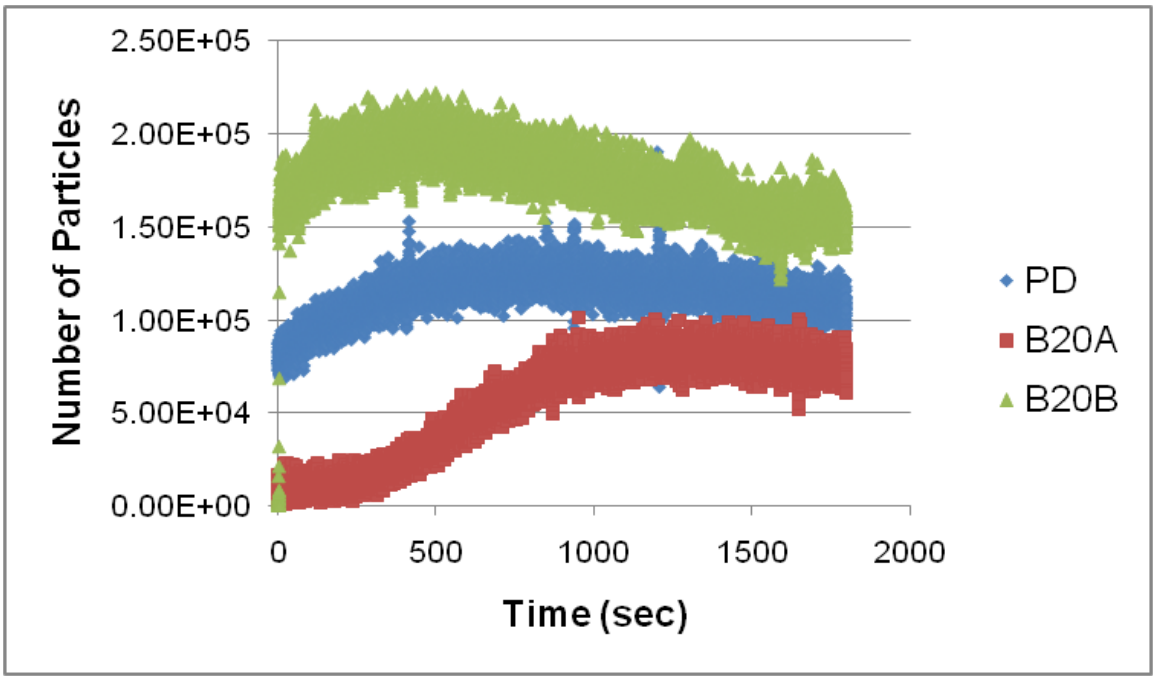

Figure 38: Particle emissions versus time for MD2.

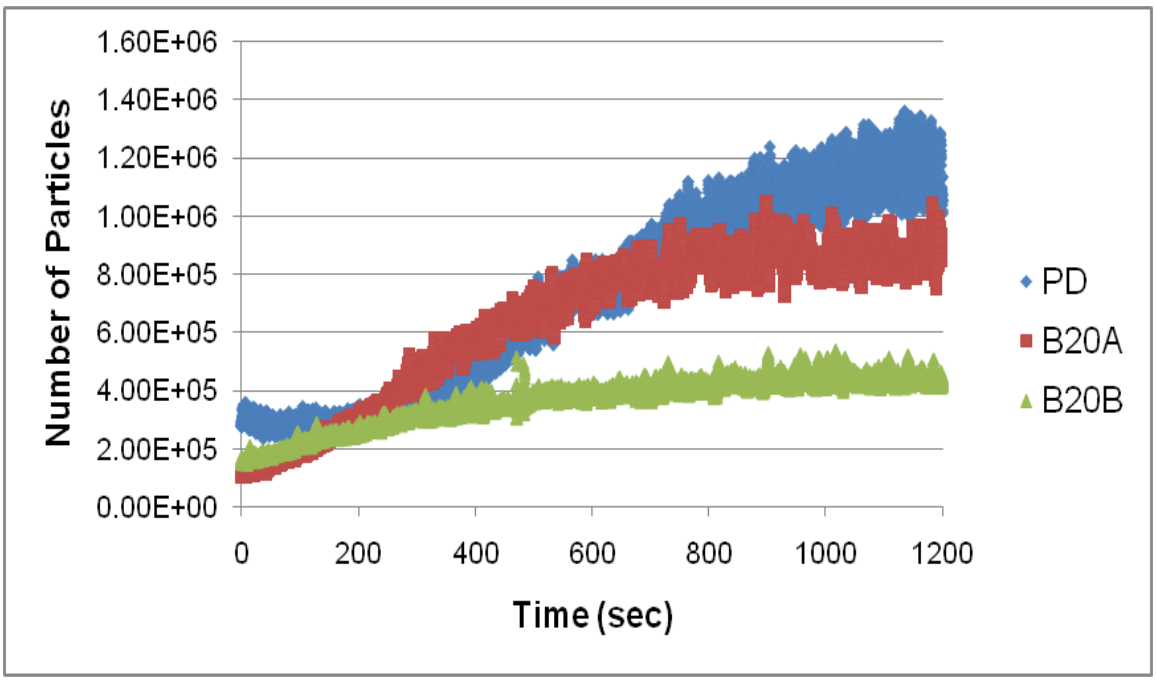

Figure 39: Particle emissions versus time for MD3.

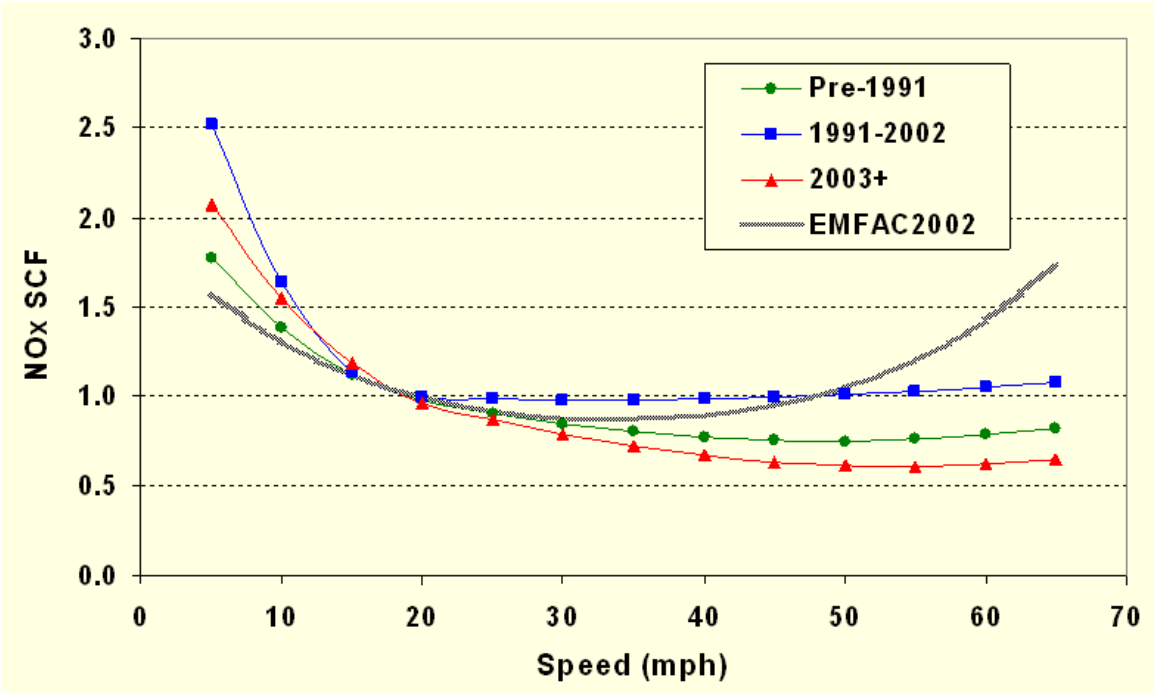

Figure 40: NO_x speed correction factor for EMFAC [90].